

ORNL-TM-4141

LOCKHEED MARTIN ENERGY RESEARCH LIBRARIES



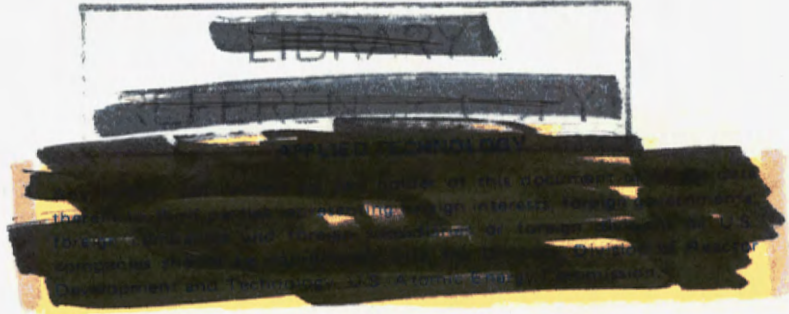
3 4456 0451406 9

cy. 64

AQUEOUS FUEL REPROCESSING QUARTERLY REPORT FOR PERIOD ENDING DECEMBER 31, 1972

W. E. Unger
R. E. Blanco
D. J. Crouse
A. R. Irvine
C. D. Watson

DISTRIBUTION LIMITED BY
AND AEC CONTRACT



193393

OAK RIDGE NATIONAL LABORATORY
CENTRAL RESEARCH LIBRARY
DOCUMENT COLLECTION
LIBRARY LOAN COPY
DO NOT TRANSFER TO ANOTHER PERSON
If you wish someone else to see this
document, send in name with document
and the library will arrange a loan.
UCN-7969
(3 3-67)



OAK RIDGE NATIONAL LABORATORY
OPERATED BY UNION CARBIDE CORPORATION • FOR THE U.S. ATOMIC ENERGY COMMISSION

This report was prepared as an account of work sponsored by the United States Government. Neither the United States nor the United States Atomic Energy Commission, nor any of their employees, nor any of their contractors, subcontractors, or their employees, makes any warranty, express or implied, or assumes any legal liability or responsibility for the accuracy, completeness or usefulness of any information, apparatus, product or process disclosed, or represents that its use would not infringe privately owned rights.

ORNL-TM-4141
UC-79c - Fuel Recycle

Contract No. W-7405-eng-26

CHEMICAL TECHNOLOGY DIVISION

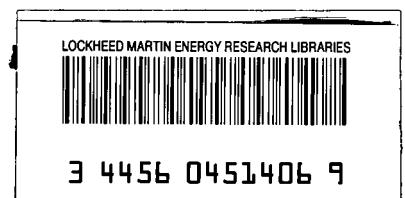
AQUEOUS FUEL REPROCESSING QUARTERLY REPORT
FOR PERIOD ENDING DECEMBER 31, 1972

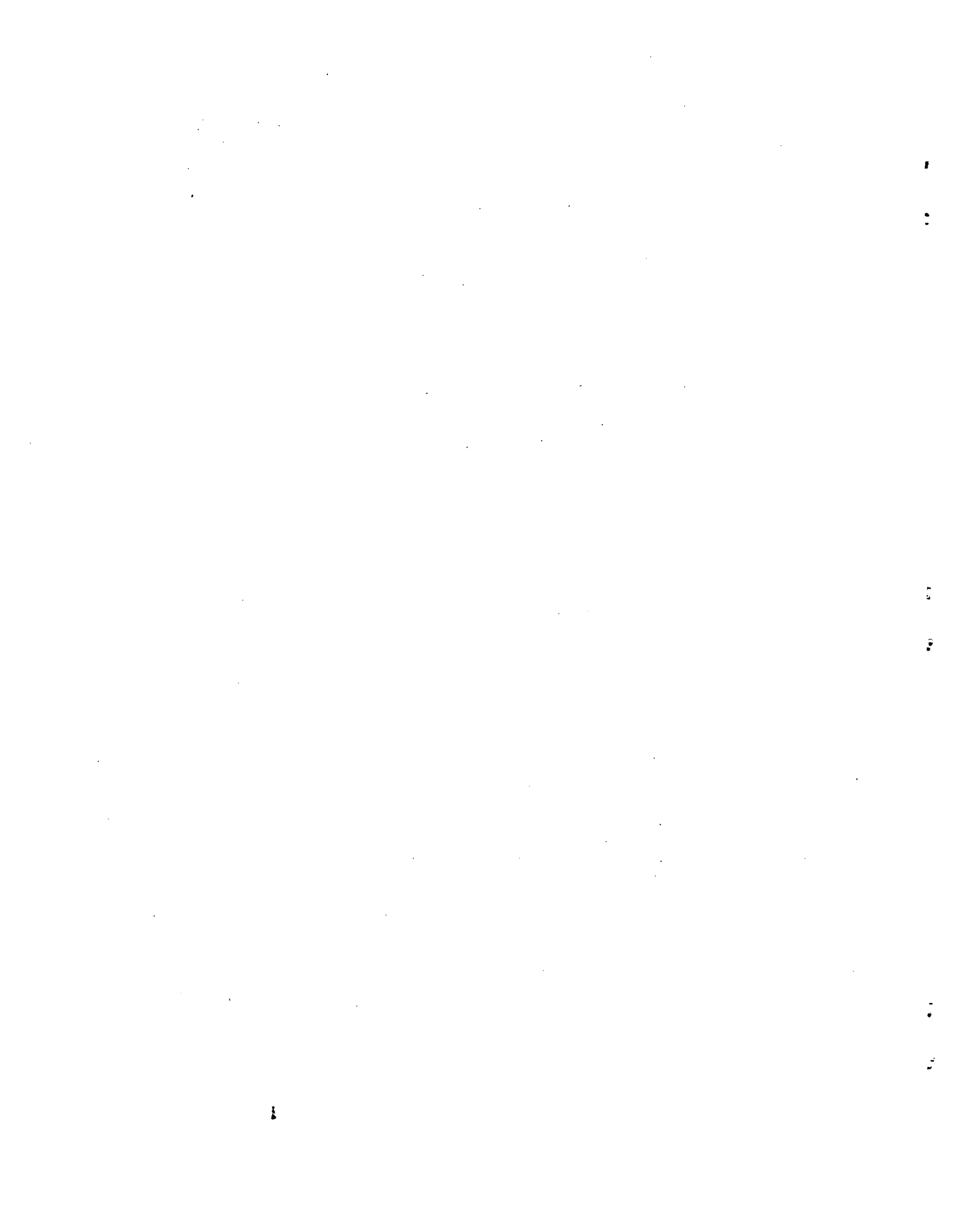
W. E. Unger, R. E. Blanco, D. J. Crouse,
A. R. Irvine, C. D. Watson

APRIL 1973

NOTICE This document contains information of a preliminary nature and was prepared primarily for internal use at the Oak Ridge National Laboratory. It is subject to revision or correction and therefore does not represent a final report.

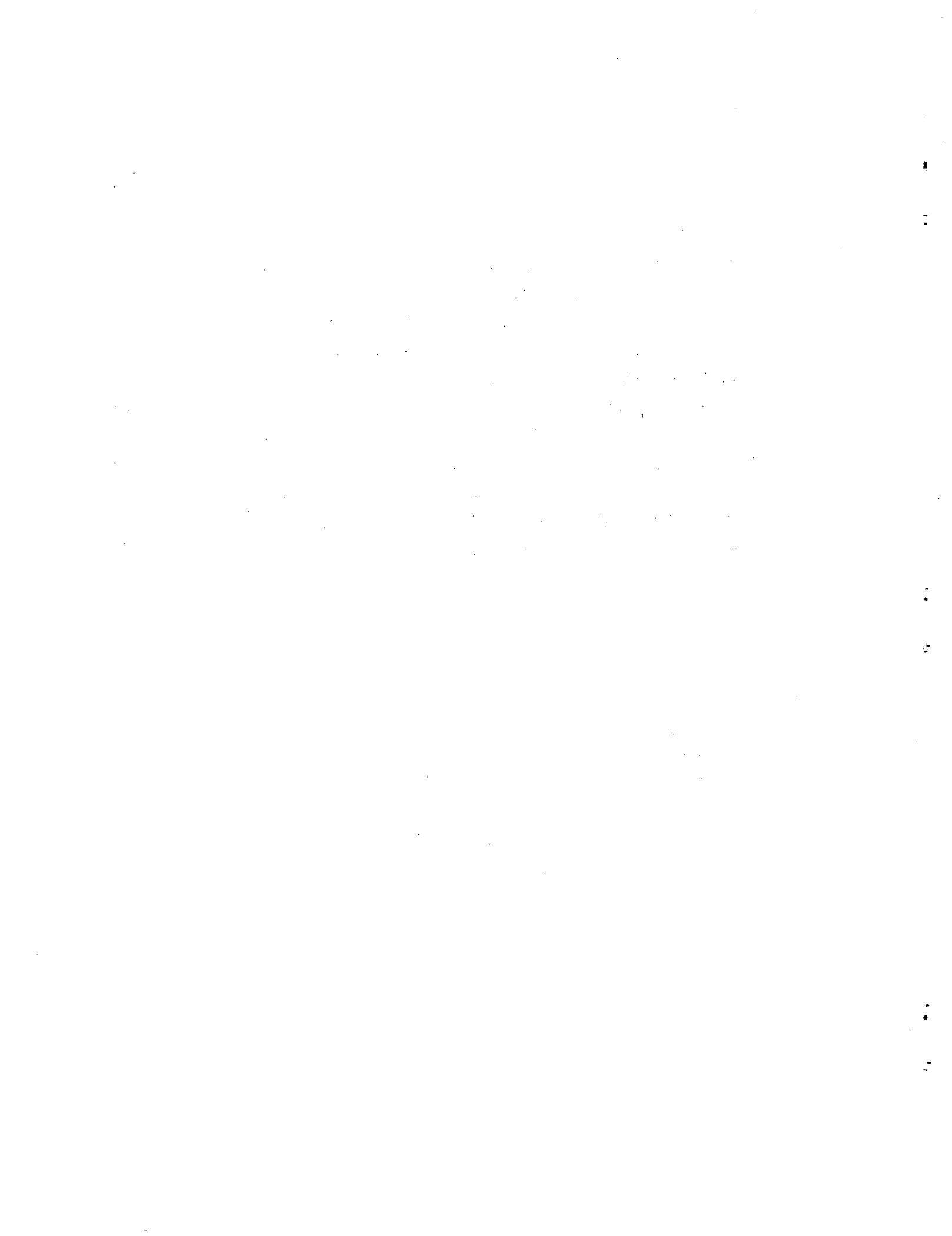
OAK RIDGE NATIONAL LABORATORY
Oak Ridge, Tennessee 37830
operated by
UNION CARBIDE CORPORATION
for the
U.S. ATOMIC ENERGY COMMISSION





CONTENTS

	<u>Page</u>
HIGHLIGHTS	1
1. Shipping (Task 1).	2
2. Receiving and Storage (Task 2)	7
3. Head-End Processing of LMFBR Fuels (Task 3).	8
4. Volatile Fission Product Removal (Task 4).	13
5. Dissolution (Task 5)	16
6. Feed Preparation (Task 6).	21
7. Solvent Extraction (Task 7).	27
8. Plutonium Purification (Task 8).	27
9. Waste Treatment and Storage (Task 9)	27
10. Off-Gas Treatment (Task 10).	27
11. Engineering Studies (Task 11).	53



AQUEOUS FUEL REPROCESSING QUARTERLY REPORT
FOR PERIOD ENDING DECEMBER 31, 1973

HIGHLIGHTS

Calculations indicate that a neutron thermal shield of practical design can serve to reduce the rate of temperature rise in a large scale cask sufficiently that after 10.4 hours exposure fire, the maximum temperature in the containment structure will be only ~ 500°F. (Sect. 1.9)

Irradiation to ~ 100,000 MWd/ton decreased the amount of plutonium that was not dissolved in 8 M HNO₃ from 15% (unirradiated pellets) to about 2%. (Sect. 5.1)

Addition of Ce⁴⁺ to dilute nitric acid increased the rate of dissolution of PuO₂ microspheres by several orders of magnitude over the rate obtained with HNO₃ alone. (Sect. 5.1)

1. SHIPPING (TASK 1)

(A. R. Irvine, C. D. Watson, L. B. Shappert, J. H. Evans,
D. S. Joy, W. C. Stoddart, G. A. West, and D. E. Willis)

The objective of Task 1 is to ensure that an economic and safe method of shipment of LMFBF spent fuel will be available when needed for transport of fuel from the demonstration and early commercial LMFBF's. The work involves analytical studies of the various facets of the problem; design, construction, and test of components, and of assemblies; and preliminary design of prototype casks.

The principal thrust of this effort is directed toward establishing that low-vapor-pressure liquid coolants can be adequately contained under conditions at least as stringent as those stipulated in the applicable regulations. In addition, the heat transport phenomenon inside a liquid-filled system is being studied. Experiments and calculations have demonstrated the overwhelming superiority of liquid sodium to gas and solid coolants from the standpoint of heat transport.

Reportable accomplishments include the following:

1.1 Heat Dissipation Studies and Tests

Fabrication of a new tube bundle for the electrically heated mockup of a fuel subassembly was completed. It has been transferred from the fabrication shop to the test facility.

A new surge tank for the single assembly mockup has been designed and parts have been ordered. This unit is needed because the thermal expansion of organic fluids is greater than that of sodium, which was used in previous tests. All drawings needed for fabrication, installation, and operation of this equipment with Dowtherm have been completed.

1.3 Cask Integrity Studies and Tests

A final report has been issued by Gray Tool Company which deals with stresses in a cask closure seal plate. The report indicates that a satisfactory system can be designed without difficulty. The report was prepared under contract with UCCND.

Two 1/6 scale LMFBR shipping cask models which were impact tested earlier have been visually inspected for damage to the cask head liners. None was found. Earlier helium mass spectrometer leak detector tests had been inconclusive because of the presence of contaminants. The sacrificial, energy-absorbing head retainers have been replaced and the models are now ready for additional impact testing.

We have taken steps to improve the reliability of the cask impact testing equipment. Items involved are: (a) the cask release mechanism, (b) the oscilloscope triggering mechanism (used in determining the duration, form, and magnitude of deceleration), and (c) means for determining peak deceleration. The third item involved the design, fabrication, and calibration of a mechanical accelerometer which employs a solid lead cylinder that is deformed under stress. The second item has been satisfactorily proof tested, but the remaining two have not yet been qualified for test use.

Because the data concerning helium holdup and release from metal surfaces coated with a dry film lubricant was somewhat ambiguous, two small Grayloc seal rings coated by the manufacturer with Everlube 812-3 were tested. These rings have a surface area of $\sim 20 \text{ in.}^2$. The release rate from these surfaces after having been immersed in helium for 30 min was $\sim 5 \times 10^{-8} \text{ cm}^3/\text{sec}$ initially and reduced to $\sim 1 \times 10^{-8} \text{ cm}^3/\text{sec}$ after 30 minutes under vacuum. After 1 hr under vacuum the rate of release was $\sim 5 \times 10^{-9} \text{ cm}^3/\text{sec}$. In a full diameter ($\sim 9 \text{ in.}$) closure, the area coated with a dry film lubricant and exposed to the test area could be reduced to $\sim 3 \text{ in.}^2$. Hence, the evolution rate from the lubricant would be in the range of $10^{-9} \text{ cm}^3/\text{sec}$; this should be acceptable.

The design of a prototype cask access port and its actuating tools was essentially completed. Work was terminated after a reduction in the effort devoted to this task.

Further investigation of thermal stresses in an 18 assembly LMFBR cask has been made. Stresses described in a previous progress report¹ were based on a stress free temperature of 0°R . This base temperature was specified because of the premise that if any body originally stress free at any base temperature is raised to any other uniform temperature and no restraints are imposed on the motion of the body, the body will be stress free at the new temperature. Consequently, the significant point is not so much the base temperature as the temperature distribution that develops in the body when heat is being transferred through it. The magnitude of the stress which occurs in the body is related to the temperature gradient established between the point of interest and a point possessing the mean temperature of the body.

The last reported case given on p. 4 of ref. 1 having a stress free temperature of 0°R was used as the basis, indicated as case 1 in Table 1-1. The stress free temperature was changed to 460°R (0°F) and 750°R (290°F); the resultant stresses are reported in Table 1-1 as cases 2 and 3.

Table 1-1

Case No.	Stress Free Temperature	Axial (psi)	Peak Stresses	
			Maximum In-Plane (psi)	Minimum In-Plane (psi)
1	0°R	-29,800	11,700	-30,500
2	460°R	-34,300	11,500	-35,500
3	750°R	-34,500	11,400	-35,900

The maximum in-plane stress varies less than 4% between cases while the minimum in-plane stress varies approximately 15%. The axial stress, which occurs because the cask was restrained from growing lengthwise, increases about 16% as the stress free temperature increases.

In an attempt to bracket the actual thermal stresses that exist in the cask during operation, both plane stress and plane strain conditions were imposed on the cask which has a stress free temperature of 460°R. These terms are defined as follows:

Plane Stress

A condition of plane stress exists relative to a plane in a body when the three stress components (normal and shear) associated with a perpendicular to the plane are all zero. The state of stress is then fully defined by the three in-plane components of stress.

Plane Strain

A condition of plane strain exists relative to a plane in a body when all points in the plane prior to loading remain in a plane after loading.

A condition of plane stress would thus be expected to exist in a thin plate loaded only by in-plane loading. A condition of plane strain would be expected in a body whose characteristic dimension normal to the plane is large and loading is independent of position along this direction.

The cask body would then not be in exactly plane stress or plane strain but would more nearly resemble plane strain. A comparison of the stress components changing only the plane stress/plane strain assumption is presented in Table 1-2. Both cases are based on a stress-free temperature of 460°R.

Table 1-2

Case No.	Stress Condition	Axial (psi)	Maximum In-Plane (psi)	Minimum In-Plane (psi)
2	Plane strain	-34,300	11,500	-35,500
4	Plane stress	0	7,900	-25,000

These stresses do not all occur at the same geometric location so their direct combination would be considered conservative.

The results of the analysis indicate that thermal stresses which occur during operation of the LMFBR cask are within reasonable bounds and do not present any difficulties.

Miscellaneous (Task 1.9)

Neutron Shield Development

Analysis of data and preparation of a report pertaining to a test of a simulated neutron shield section is continuing. Machine calculations have been made which indicate that an 18 assembly steel cask carrying 30-day-cooled fuel could exist for 10.4 hours in a 1475°F fire before all the hydroxide salt melted. At this time the maximum temperature of any of the steel gamma shielding (cask structure) is calculated to be 502°F. The basis for the calculations was an emissivity-absorptivity coefficient for the two interior surfaces of 0.1 and that the salt is retained within the inner container until all the salt is melted.

Studies of the Reactions of Dowtherm with Metallic Sodium

Studies were continued on the chemical feasibility of using Dowtherm as a coolant during transport of spent LMFBR fuels. Previously reported work includes information from the literature² on the reactions between sodium metal and diphenyl oxide, results of preliminary tests of the

reactions between sodium and mixed biphenyl--diphenyl oxide (Dowtherm A), and more detailed tests³ of the reaction between sodium metal and biphenyl alone. More recent tests were directed toward (1) determining if the reaction products resulting from biphenyl alone or mixed biphenyl--diphenyl oxide will adhere to sodium-coated stainless steel surfaces and (2) further determinations of the characteristics of the products from the mixed Dowtherm A.

For the adhesion tests, small coupons of stainless steel were coated with a thin layer of sodium metal by immersion in molten sodium at a temperature $> 500^{\circ}\text{C}$ in an inert atmosphere dry box. These coated coupons were then heated in an inert (argon) atmosphere to $\sim 250^{\circ}\text{C}$ with (1) biphenyl alone or (2) Dowtherm A for ~ 13 hours. With biphenyl alone, the light-colored surface of the sodium quickly darkened as the reaction products (most likely a mixture of various condensed polyphenyls) built up on the sodium surface to which they adhered very tightly. This coating prevented complete reaction of all sodium, since active sodium was shown to be present underneath the outer black layer. The polyphenyls and active sodium could only be removed from the stainless steel with hard mechanical scraping. This removal difficulty, together with the previously determined fact that the sodium acts mainly as a catalyst (and hence could result in complete decomposition of biphenyl if in extended contact with it), leads to the conclusion that use of the pure compound is impractical. In the case of mixed biphenyl--diphenyl oxide, the reactions of sodium are faster than with biphenyl, and, at higher temperatures, final products are formed such as sodium oxide, sodium phenolate, higher phenols, benzene, tars, etc. Since the sodium is consumed in these reactions, the decomposition should be limited by the amount of sodium present. In the adhesion tests with the mixed coolant, the reaction products did not adhere to the sodium-coated stainless steel. Instead they partially dissolved in the reactant mixture turning it dark red-brown, while the insoluble portion settled to the bottom of the reaction flask. These solids were partially soluble in xylene and in methyl alcohol. In addition, a low-boiling product, probably benzene, condensed on the cool surfaces of an outlet tube.

In subsequent tests with sodium and biphenyl--diphenyl oxide, the organic mixture was first purified by preliminary reaction with sodium and vacuum distillation. Portions of this purified Dowtherm mixture were then contacted with a quantity of sodium metal equal to 0.5 wt % of the Dowtherm at a temperature of $\sim 250^{\circ}\text{C}$ and at $\sim 100^{\circ}\text{C}$ for ~ 7 days. At the higher temperature the mass quickly darkened with large amounts of black (or dark brown) solids forming. Benzene added to the cool reaction mixture dissolved almost all the solids to give a black solution. At the lower temperature little reaction appeared to occur with formation of only small amounts of light-colored material. Apparently, most of the sodium was unreacted. We plan to determine the amount by reaction with benzyl chloride. A similar determination will be made on the products from high temperature reaction, plus a determination of the amount of reacted sodium.

These results with the Dowtherm mixture point to several potential problems. One is that at the cooler parts of a fuel element, all sodium would not react and thus would probably require another method to destroy

it. Another is that phenylsodium, which is reported² to be an intermediate product in reaction with the diphenyl oxide, could be a source of an autoignition if it should come in contact with air as a result of malfunction and loss of the inert gas over the Dowtherm. This, in conjunction with some low-flash-point benzene, could result in a fire hazard. In any case, the decomposition of Dowtherm will probably necessitate its periodic replacement.

References

1. W. E. Unger et al., LMFBR Fuel Cycle Studies Progress Report for September 1972, No. 43, ORNL-TM-4016 (November 1972).
2. a. Paul Schorigin, "The Decomposition of Ethers by Metallic Sodium," Bev. 56, 176-86 (1923).
b. Burge Muller, "Decomposition of Diphenyl Ether," Bev. 69, 2171-2 (1936).
3. a. W. E. Unger et al., LMFBR Fuel Cycle Studies Progress Report for July 1972, No. 41, ORNL-3952 (September 1972).
b. Ibid. for August 1972, No. 42, ORNL-3993 (October 1972).

2. RECEIVING AND STORAGE (TASK 2)

This task is concerned with the means for rapid, effective, economical, and safe operation of receiving and storage facilities for LMFBR fuels.

No work was performed on this task.

3. HEAD-END PROCESSING OF LMFBR FUELS (TASK 3)

(C. D. Watson)

The objectives of this task are to develop economic head-end processing steps, in preparation for Purex recovery methods, for long- and short-decayed fuels.

3.1 Decay Heat Dissipation (Task 3.1)

(R. L. Cox and S. D. Clinton)

A report, ORNL-TM-3773, "A Computer Program for Calculating Temperatures Attained by LMFBR Fuels From Decay Heat Emission" by R. L. Cox, is in rough draft and is being processed through our editorial review procedure. A brief summary of the report follows:

In the handling and reprocessing of spent LMFBR nuclear fuel assemblies producing heat by radioactive decay emission, it is necessary to know the temperatures which may be expected in the various reprocessing steps in order to properly design the equipment and provide for auxiliary cooling, if required. For this purpose, a computer program, HEX, has been developed as a means of calculating conservatively the temperature distributions in hexagonal LMFBR fuel assemblies. In this program, it is assumed that heat transfer within the array is by thermal radiation interchange between rods. As a necessary first step, black body view factors are derived for parallel cylinders on an equilateral triangular pitch. These view factors are then used in the HEX code to calculate the temperatures in any size hexagonal array which may be of interest as a function of the emissivities of the surfaces, pitch-to-diameter ratio of the rods, and heat generation rates. Solution is by the net radiation method with one equation for each surface involved with proper account taken of the possible energy interchanges between the various surfaces. The resulting calculated temperature values may then be used appropriately in the design of reprocessing facilities and processing equipment. Sample calculations are presented in the report as an aid to the prospective user.

The HEX code was first used sometime ago to calculate steady state and unsteady state temperatures in Atomic International (AI) Reference, AI Follow-On, General Electric Follow-On, and Fast Test Reactor core assemblies. These initial calculations are reported in ORNL-TM-2906, "A Study of the Reprocessing of Spent Fast Test Reactor Fuel (and Other LMFBR Fuels) in the Nuclear Fuel Services Plant", C. D. Watson, A. R. Irvine, et. al., August 1971.

Thermal Conductivity Studies (S. D. Clinton and R. L. Cox)

A report, ORNL-TM-3772, "The Effective Thermal Conductivity of Sheared Prototype LMFBR Fuels", S. D. Clinton and R. L. Cox, has been completed and is now at the printers. The abstract from this report follows:

"During the recovery of uranium and plutonium from irradiated LMFBR fuels by the mechanical shear-leach and aqueous Purex process, the volume of accumulated sheared fuel may be restricted by heat transfer limitations. The calculation of temperature gradients within a given volume of spent sheared fuels requires a knowledge of the effective thermal conductivity of the chopped fuel pieces. In this study, the effective thermal conductivities of 11 prototype systems were measured experimentally as a function of temperature. The experimental measurements were made at steady-state conditions using the technique of radial heat flow in a hollow cylinder. The prototype sheared systems ranged from metal-clad porcelain or unirradiated urania to empty stainless steel hulls in either an argon or air atmosphere. The measured thermal conductivities for each system could be correlated as an exponential function of temperature with an average deviation of only $\pm 4.1\%$ over the temperature range 200 to 1400°F. For stainless-steel-clad urania pellets that simulate sheared fuel from the LMFBR core region (0.305 in. diam by 1 in. long), the expression for the effective thermal conductivity was as follows:

$$k(\text{Btu/hr-ft-}^\circ\text{F}) = 0.109e^{0.00168T(^\circ\text{F})}."$$

Similar equations for the other prototype systems are included in the main body of the report.

3.2 Dismantling of Multitubular Assemblies (Task 3.2)

(G. A. West and D. E. Willis)

The dismantling of fuel subassemblies is desirable to remove the unfueled end adapters, gas plenum, shroud and spacer wire waste metal from the subsequent processing steps and to produce lamina or bundles of de-shrouded fuel rods for shearing. In its simplest forms, the disassembly operation would be (1) comprised of the cropping operation to remove end

adapters and/or the gas plenum and (2) circumferential slitting of the shroud at the appropriate end adapter and the withdrawal of all fuel rods from the shroud using the end adapter as a handle.

The processing methods currently being evaluated are (1) removal of the end hardware by either transverse cutting with a plasma torch or with a pincer type shear and (2) removal of the shroud by cutting through the hexagonal corners with either a plasma-arc torch or a high speed abrasive belt grinder. Cutting with the plasma-arc torch has been successfully demonstrated on short prototype sheaths (2 to 6 ft lengths). The guidance probes for the plasma torch were also demonstrated successfully in controlling the torch position so that the fuel rods were not damaged.

Recent cutting tests with the plasma torch in which the hexagonal corners of an AI prototype subassembly were cut longitudinally show that a second cutting pass made over a previous cut almost always results in breaching of the cladding and spalling of fuel. The apparent reason for this phenomenon appears to stem from the close tolerance requirements of the torch to the workpiece to maintain a cutting plasma and the thick coating on the first cut. We will continue to investigate the problems associated with making an acceptable second cutting pass over an old cut.

In future tests, we will also determine the effect of the presence of sodium on the performance of the plasma torch and also the effect the plasma will have on UO_2 pellets if they are contacted momentarily during the cutting operation.

3.3 Shearing (Task 3.3)

(G. A. West, J. C. Rose and D. E. Willis)

A total of twenty sodium logged fuel rods were successfully sheared singularly in the multirod shear in an argon atmosphere to produce experimental material for the Internal Sodium Deactivation Program. The rods were sheared into 0.5 and 1.0-inch lengths. The prototype fuel sheared was clad in 304 stainless steel tubing; 0.305-in. OD x 0.015-in. wall, filled with 0.270-in. OD UO_2 pellets with a total of ~2.75 grams per rod of metallic sodium around and atop the UO_2 pellets. The shearing operation was completely normal with no indication of any change caused by the presence of metallic sodium.

A short section of a 217 rod prototype LMFBR subassembly was sheared with the modified elongated shear blade in the ORNL 250-ton shear. The sheared material did not jam in the area between the teeth; however, shroud breakup was not as successful as with the original blade design. The blade used had been modified by the insertion of a tapered blade section in the relief area between the top and bottom teeth.

In an additional scoping test with the bundle shear, an attempt was made to produce terminal sheared pieces of fuel 1-in. long. An AI core prototype (porcelain filled tubes) with an attached 14-inch long gas plenum section compacted with 50 or 60 tons force applied on one of the hexagonal flats was used in the test. The gag or restraining force exerted by the ORNL 250-ton shear is only ~26-tons. This gag force was not sufficient to prevent the fuel tubes from moving slightly forward at each shear stroke since a force of 50 to 60 tons is required for positive gag holding. The results of shearing at the terminal fuel portion of the subassembly showed that the test was successful but that there was some mixing of flattened empty (plenum) tubes with the sheared filled tubes in about a 4-inch section because of the pull and forward displacement into the shear of some of the fuel rods by the shear blade. However, there was no porcelain observed in the flattened and sheared plenum sections. It had been assumed that some UO₂ powder or fragments could be dislodged into the plenum when shearing irradiated fuel. However, this is not likely to occur if the gas plenum section is compacted sufficiently to completely flatten and close the tubular cladding.

Exploratory shearing tests were also made with the ORNL 250-ton prototype shear to determine the feasibility of shearing a deshrouded LMFBR fuel bundle comprised of approximately 217 wire wrapped rods in the uncompacted mode and compared to the shearing of a ductile uncarbured subassembly. Three shear blades were used in the tests. A 20-inch long prototype fuel bundle previously subjected to an incomplete carburization process was deshrouded using the plasma-arc technique of cutting opposite corners of the hexagonal shroud longitudinally. The 217 deshrouded fuel rods were not compacted prior to shearing but were restrained by a gagging force of approximately 25 tons.

The exploratory feasibility shearing tests compared (1) the product produced by three different blade configurations, and (2) the effectiveness of a normal gagging or holding system in restraining the uncompacted loose rods.

Both of our two newer shear blades, designed to break the LMFBR hexagonal shroud, (1) an elongated stepped blade and (2) a straight sharks tooth blade, produced ~6% more dislodged fuel and ruptured ~12% more clad than an old conventional LWR type stepped blade (Table 3-1). The rupturing of the clad is considered to be desirable in that more of the fuel is exposed to the dissolver acid.

The dual gags used (inner, oval shaped and outer, V-shaped with serrated teeth) were operated at a maximum force of ~25-tons.

The measurements of the product from shearing a ductile prototype, Atomics International Reference core (porcelain filled rods), verify that even slight carburization of rods will result in more dislodgement

of fuel. The fuel particles <2000 microns in size that were dislodged from the non-carburized subassembly was 5.7 wt. % compared to 10.4 wt. % from carburized (0.1 to 5-mil penetration) rods -- Table 3-1.

Another scouting type test was made on a prototype AI core subassembly compacted (50-ton force) without side restraints to produce an elliptical shape (2-1/4 x 8-5/8 inch, maximum dimensions). Shear tests were made with the modified elongated stepped blade on this bundle to observe the effect on shroud breakage. The shroud pieces produced were about the same lengths as those observed in other compacted configurations, i.e., 1.5 to 5-inch lengths. However, the shear force required to cut through this flattened bundle was much less than at the other shapes previously sheared.

Solids transfer studies are currently being made to determine, (1) the slip angle of the product from a single shear cut from a whole shrouded subassembly and (2) the possibility of bridging in 8-in. ID and 12-in. ID stainless steel transfer ducts.

4. VOLATILE FISSION PRODUCT REMOVAL (TASK 4)

(D. J. Crouse and C. D. Watson)

The objective of Task 4 is to develop a head-end processing method for removing tritium from the fuel prior to aqueous processing. Based on experimental work, it appears that this objective can be met by heating the oxide fuel to about 500°C in flowing oxygen or air (this treatment is termed voloxidation). Early removal of tritium from the fuel into a relatively small volume of gas is desirable to avoid large dilution of the tritium with water in the fuel dissolution step. In addition, the oxidation treatment has the advantage of converting any residual sodium in the fuel to the oxide prior to dissolution.

This quarter the release of tritium from "impregnated" unirradiated $\text{UO}_2\text{-CeO}_2$ fuel was studied in the laboratory. Preliminary voloxidation results are presented for the processing campaign with short-cooled fuel (100,000 Mwd/ton) that is now in progress. Laboratory tests indicated that internal sodium in fuel rods will not prevent efficient release of tritium from the fuel.

4.1 Volatilization from Oxide Fuels (Task 4.1)

(J. H. Goode, C. L. Fitzgerald, G. D. Davis, and O. L. Kirkland)

We are investigating the minimal conditions of time, temperature, and oxygen concentration that will remove tritium from IMFBR core and blanket materials. Previous work with irradiated specimens showed that heating in vacuum or an inert atmosphere released less than half of the tritium, while oxidation volatilized essentially all of it.¹ We recently conducted a short program of trying to impregnate tritium into non-plutonium-bearing, unirradiated pellets so that the voloxidation variables could be studied in the laboratory instead of a hot cell.

Tests² with FTR-specification UO_2 insulator pellets were not successful since the tritium did not penetrate deeply into the pellets (the outer 10% of the pellets held about 90% of the tritium) and was easily desorbed in a sweep of Ar--4% H_2 at 500°C. The impregnation procedure involved reducing the pellets in Ar--4% H_2 at 900°C, "soaking" them for 5 hr at 600-700°C in an Ar--4% H_2 --³ H_2 atmosphere, and cooling to ambient temperatures.

Pellets of $(\text{U,Th})\text{O}_2$ and $(\text{U,Ce})\text{O}_2$ were successfully impregnated with tritium by heating them in Ar--4% H_2 --³ H_2 . These materials provide lattice vacancies for the tritium, and we were able to introduce sufficient quantities of tritium into the pellets to allow study of the effects of voloxidation variables on tritium removal. Incremental dissolving tests showed that the tritium was dispersed uniformly throughout the pellets. Also, only adsorbed surface tritium was desorbed by a helium purge at 500°C for 4 hr.

The effects of temperature and time on tritium removal were studied using the $(\text{U,Ce})\text{O}_2$ pellets. Oxygen concentration was constant at 3% at temperatures of 300, 390, and 480°C for periods of 4 and 8 hr (Table 4-1).

Table 4-1. Volatilization of Tritium from
(U_{0.8}Ce_{0.2})O₂ Pellets in Flowing 3% O₂--97% N₂

Temperature (°C)	Tritium Volatilized (% of initial)	
	4 hr	8 hr
300	31	48
390	84	-
480	>94 ^a	-

^aResidual tritium was close to background.

Less than half (48%) of the ³H was removed from the pellets at 300°C in 8 hr. However, 84% was removed at 390°C in 4 hr, and more than 94% (approximate limit of detection) was volatilized at 480°C in 4 hr.

Hot Cell Studies. - Irradiation capsule 43-119, containing four 7.5-in.-long (U,Pu)O₂ fuel rods intended for short-cooled processing tests, was discharged from the ETR on October 23, 1972. The capsule was delivered to ORNL on November 6, and was examined, photographed, punctured, and sectioned for metallography. The processing tests were started after the fuel had cooled for about 35 days. Information is being obtained on volatile fission product removal, dissolution of the fuel, and removal of iodine from the dissolver solution. The series of experiments is still in progress, and only preliminary results are available.

Irradiation of the stainless steel-clad (U_{0.75}Pu_{0.25})O_{1.98} FTR dissolution reference pellets to a nominal 100,000 MWd/ton released about 33% of the ⁸⁵Kr and about 1% of the ¹³³Xe fission gases to the gas plenum. The diffusion coefficient of the xenon (1.90 Å diam) is an order of magnitude less than that of the krypton (1.69 Å diam) which may account for some of the difference in gas release; the large difference in half-lives of the two isotopes would also favor preferential ⁸⁵Kr release. The linear heat rating (kW/ft) of the rods has yet to be calculated; this will provide the reference point for comparison of the gas release with other rods in the irradiation series.

Only fragmentary analytical data have been returned from the first set of four runs. These preliminary data indicate that 0.5- and 1.0-hr vol-oxidations (in air at 480°C) released only about 2/3 of the tritium; a 4-hr treatment released more than 93% of the tritium, ~39% of the krypton, and ~10% of the xenon.

Reactions of Tritiated Water with Sodium and UO₂ During Voloxidation
(D. E. Horner and D. J. Crouse)

Prior to processing, IMFBR fuel assemblies will be cleaned of external sodium. However, it is anticipated that a significant quantity of sodium

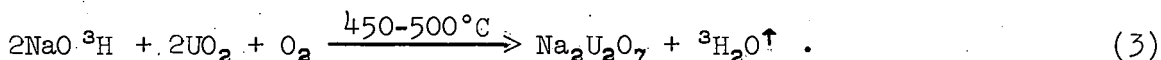
will have leaked into some of the fuel pins during irradiation and will not be removed in the cleaning step. Some of this sodium might be expected to react with tritium to form sodium tritide inside the fuel pin during irradiation; the sodium tritide could then react to form tritiated sodium hydroxide during voloxidation,



Presumably, the voloxidation treatment would convert the balance of the sodium in the logged pins to sodium oxide and the tritium gas in the system to tritiated water; reactions of these compounds could also result in formation of some tritiated sodium hydroxide,



Conceivably, these reactions could prevent complete removal of tritium in the voloxidation step. We have considered, however, that the tritiated sodium hydroxide probably would react with uranium oxide to liberate the tritium as tritiated water,



Preliminary experiments indicate that reaction (3) would indeed occur.

An initial test was run to confirm that, under voloxidation conditions, sodium metal would react with oxygen and tritiated water vapor to form tritiated sodium hydroxide. In this test, a boat containing a known amount of sodium metal was placed in a tube furnace. Air was bubbled through tritiated water at room temperature and then passed through the furnace for 0.5 hr at 475°C. The contents of the boat were then dissolved in water, and the tritium concentration in the solution was determined. Under these conditions, the amount of tritium trapped by the sodium was about 70% of the amount expected on the basis of Eq. (2) and assuming that the hydrogen/tritium ratio was the same in the tritiated sodium hydroxide as in the tritiated water.

A second experiment was then run in which a known weight of sodium metal was converted to tritiated sodium hydroxide as before. Uranium dioxide microspheres (~8 moles per mole of Na) were then added to the boat, and heating at 475°C was continued for 5 hr while passing air that had been bubbled through normal (nontritiated) water through the furnace. At the end of the test the solids in the boat included a small amount of reddish-brown material (presumably sodium uranates). Leaching of this material with water to dissolve unreacted tritiated sodium hydroxide showed that essentially no tritium was present. A third test was then made which was identical to the second test except that dry air rather than wet air was passed through the furnace after addition of the UO₂. As in the second experiment, no significant amount of tritium (<0.1% of that found in the first test) was found in the reaction boat.

These experiments indicate that reaction (3) will proceed under voloxidation conditions, thereby preventing retention of tritium by internal sodium in the fuel rods. Some additional tests will be made with sheared sodium-bonded, UO_2 -filled rods.

References for Section 4

1. Chem. Technol. Div. Annu. Progr. Rep. March 31, 1972, ORNL-4794, p. 19.
2. W. E. Unger et al., LMFBR Fuel Cycle Studies Progress Report for September 1972, No. 43, Sect. 4.1, ORNL-TM-4016.

5. DISSOLUTION (TASK 5)

(D. J. Crouse and C. D. Watson)

The objective of Task 5 is to ensure that LMFBR fuels can be dissolved in nitric acid with high metal recoveries. Since the dissolution characteristics of the fuels can vary widely depending on their plutonium content, method of preparation, and irradiation histories, extensive leaching data are being obtained to define the effects of the many variables. A thorough understanding of iodine chemistry in the dissolver system is needed as a guide for providing effective iodine control. The dissolver equipment must be designed and operated within rather narrow limitations imposed by criticality control and off-gas considerations. It appears that satisfactory solution of these problems can best be accomplished using continuous dissolving methods and this approach is being emphasized. Evolution of a successful dissolver will require development of equipment for dependably moving the sheared stainless steel hulls and other solids through the system, and development of seals for isolating the system to prevent excessive inleakage of diluent gases.

This quarter dissolution tests with UO_2 - PuO_2 fuel specimens showed that irradiation to 100,000 MWd/ton decreased the amount of insoluble plutonium about tenfold compared to the unirradiated fuel. Addition of Ce^{4+} to dilute nitric acid solutions increased the instantaneous dissolution rates for PuO_2 microspheres by several orders of magnitude.

5.1 Dissolution of Oxide Fuels (Task 5.1)

(J. H. Goode, C. L. Fitzgerald, and O. L. Kirkland)

The initial results from the short-cooled hot cell tests (Sect. 4.1) indicate that long (34 mo) irradiation greatly improved the solubility of a rather poor grade of mechanically blended $(U,Pu)O_2$ pellets. The FTR dissolution reference pellets, fabricated in 1969 by HEDL, have been the subject of continuing study. About 16% of the PuO_2 in the as-received pellets was insoluble after 10 to 12 hr in boiling 8 M HNO_3 . Irradiation to about 20,000 MWd/ton in the ETR gave about 5% insoluble PuO_2 . The current short-cooled tests, at about 100,000 MWd/ton, are indicating that

from 1.5 to 2.7% of the PuO_2 is not dissolving in 8 M HNO_3 under similar conditions (Fig. 5-1).

Dissolution of PuO_2 Microspheres in Nitric Acid

(D. E. Horner, F. A. Kappelmann, D. J. Crouse, W. D. Bond, and R. L. Hickey)

Tests at Hanford and ORNL have indicated that, with present fabrication techniques, possibly 1 to 3% of the plutonium in irradiated LMFBR fuels may remain undissolved after a dissolution treatment with 8 to 12 M HNO_3 . Our present reference flowsheet calls for treatment of the residue with HNO_3 -HF to achieve complete plutonium recovery. We recently initiated dissolution studies with PuO_2 microspheres to define conditions required for effective dissolution of the residual plutonium. Later, these tests will be extended to include residues obtained from dissolution of a poor grade of unirradiated, mechanically blended UO_2 - PuO_2 pellets in HNO_3 .

We are particularly interested in the possibility that addition of cerium to the nitric acid may provide rapid plutonium dissolution so that use of highly corrosive fluoride can be avoided. It has been reported^{1,2} that Ce^{4+} increases the dissolution rate. Initial results have been encouraging.

The PuO_2 microspheres being used in our tests are of high density (96% of theoretical) and, therefore, particularly difficult to dissolve. So far, only instantaneous dissolution rates (IDR) over a 1.5-hr period have been measured, resulting over this period in dissolution of a maximum of 15-20% of the plutonium. Some extended dissolution tests are presently being run to obtain estimates of the time needed for total dissolution of the plutonium.

Dissolution test results obtained with HNO_3 , HNO_3 - Ce^{3+} , HNO_3 - Ce^{4+} and HNO_3 -NaF solutions are presented in Table 5-1. With 0.1 M Ce^{4+} in 4 M HNO_3 , the IDR was a factor of 10^3 higher than with 16 M HNO_3 and a factor of 3 higher than with 8 M HNO_3 --0.05 M F^- solution. Examination of the effect of varying the acid concentration in the range of 2 to 6 M while maintaining the Ce^{4+} constant at 0.1 M showed that the dissolution rate was at a maximum at about 4 M acid concentration. In another series of tests (in 4 M HNO_3), the IDR increased with increasing Ce^{4+} concentration over the range of 0.01 to 0.1 M, but the increase was less than proportional to the increase in Ce^{4+} concentration (Fig. 5-2).

It was reported in reference 2 that adding Ce^{3+} was as effective as adding Ce^{4+} in promoting plutonium dissolution. All of the tests were made, however, with boiling 16 M HNO_3 , a condition which results in rapid oxidation of Ce^{3+} to Ce^{4+} . Our tests with Ce^{3+} at lower acid concentrations (2 to 10 M) were disappointing. Although the dissolution rates were much higher than would be predicted for HNO_3 alone (using the 16 M HNO_3 data and assuming a fourth-power dependence³ on acid concentration), they were still relatively low.

Tests are now being run to determine Ce^{4+} consumption during dissolution; presumably, all of the plutonium in solution is oxidized to the

ORNL DWG. 73-1928

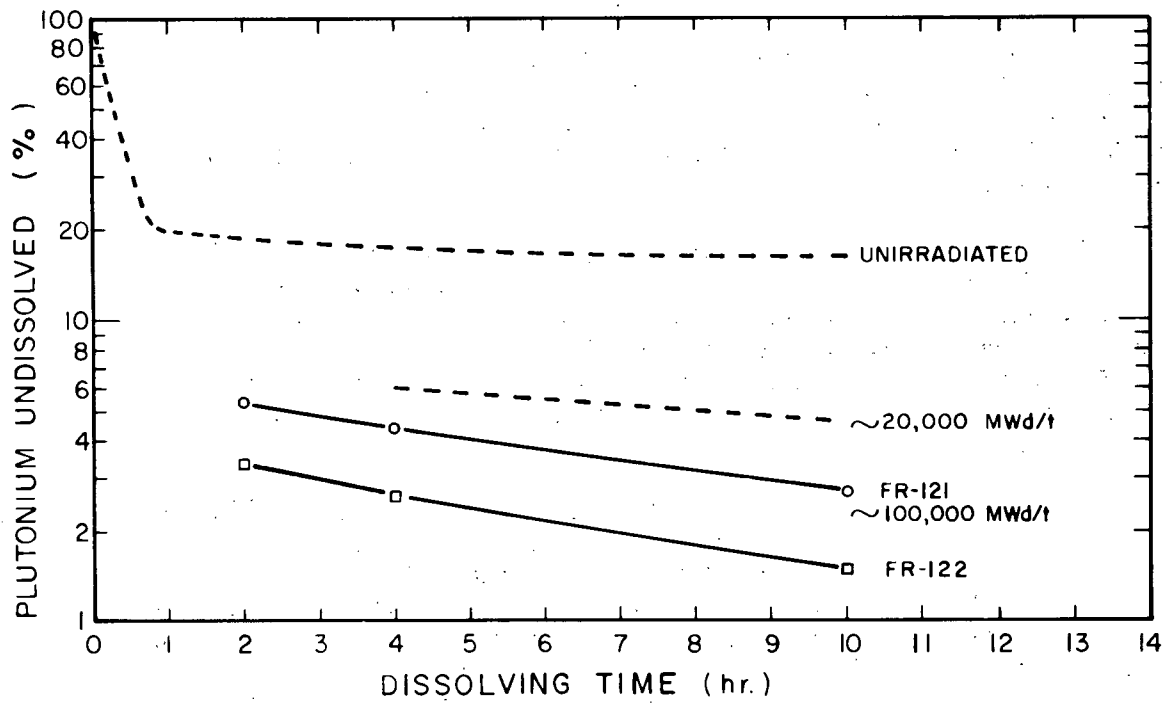


Fig. 5-1. Dissolution of $\text{UO}_2\text{-PuO}_2$ in Boiling 8 M HNO_3 . FTR dissolution reference pellets--mechanically blended $(\bar{\text{U}}_{0.75}\text{Pu}_{0.25})_{1.98}$.

Table 5-1. Dissolution Data for PuO₂ Microspheres

Procedure: ~1-g samples of PuO₂ microspheres added to 150 ml of dissolver solution at boiling temperature. Duplicate samples of solution taken at 15-min intervals for gross alpha counting. Original surface area of microspheres = 1.2×10^2 cm²/g. Density = 11.0 (96% of theoretical); particle size ranged from 149 to 177 microns.

Dissolver Solution			
HNO ₃ (M)	Ce ³⁺ (M)	Ce ⁴⁺ (M)	Instantaneous Dissolution Rate (mg cm ⁻² min ⁻¹)
14	0	0	2.4×10^{-6}
16	0	0	3.8×10^{-6}
2	0.1	0	6.6×10^{-6}
4	0.1	0	5.6×10^{-6}
8	0.1	0	3.8×10^{-6}
10	0.1	0	1.1×10^{-4}
1	0	0.1	Precipitation
2	0	0.1	1.3×10^{-2}
3	0	0.1	2.3×10^{-2}
4	0	0.01	6.0×10^{-3}
4	0	0.03	1.8×10^{-2}
4	0	0.07	3.0×10^{-2}
4	0	0.1	3.3×10^{-2}
6	0	0.1	2.4×10^{-2}
8 (plus 0.05 M F ⁻)	0	0	1.2×10^{-2}

hexavalent state with equivalent reduction of Ce⁴⁺ to Ce³⁺. In process practice, continuous reoxidation of the Ce³⁺ would probably be required to limit cerium consumption to a tolerable value. Ozone oxidizes cerium readily or, conceivably, the oxidation could be accomplished electrolytically. Tests have also been started to determine the effect of Ce⁴⁺ on the stability to corrosion of stainless steel.

References for Section 5

1. Armando L. Uriarte and Robert H. Rainey, Dissolution of High-Density UO₂, PuO₂, and UO₂-PuO₂ Pellets in Inorganic Acids, ORNL-3695 (1965).
2. U.S. Patent No. 3,005,682.

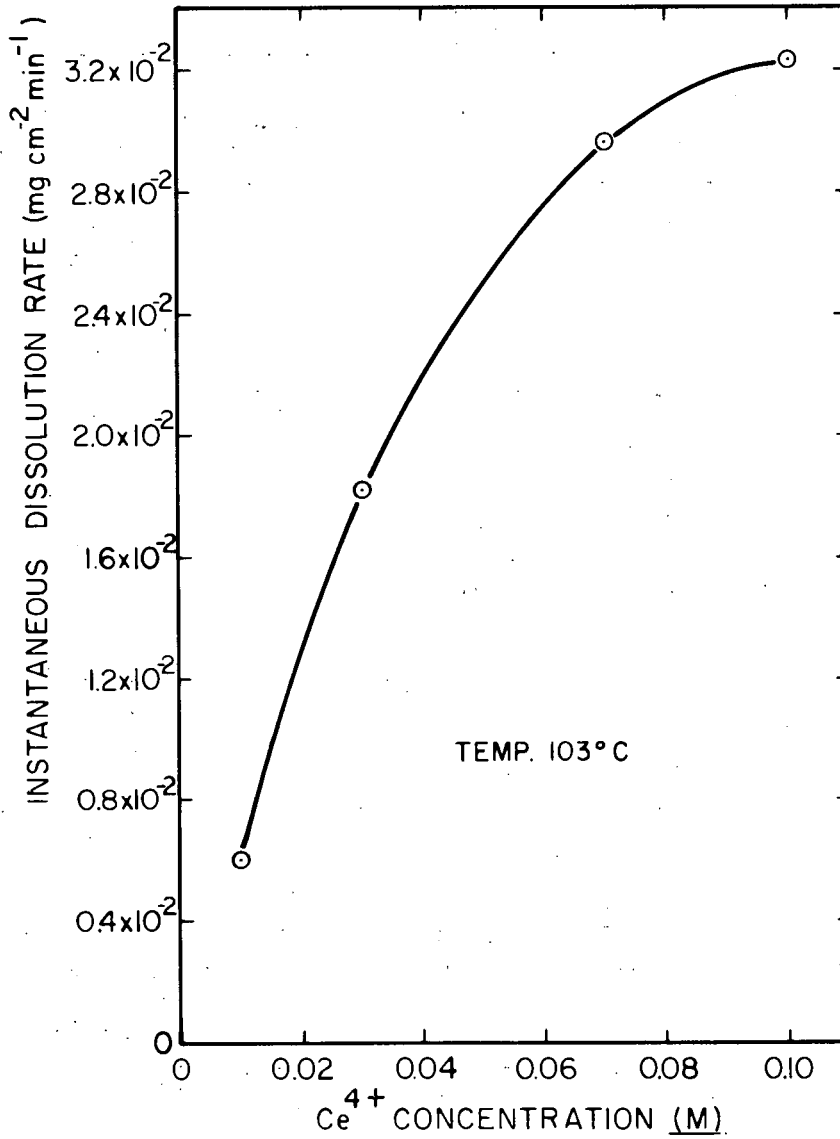


Fig. 5-2. Effect of Ce⁴⁺ Concentration on Dissolution of PuO₂ in Boiling 4 M HNO₃.

6. FEED PREPARATION (TASK 6)

(D. J. Crouse)

The aqueous feed discharged from the dissolver will contain solids (undissolved fission products, corrosion products, etc.) and will probably require clarification prior to solvent extraction. Preparation of the feed for solvent extraction also will include adjustment of the plutonium valence and the nitric acid concentration, and a treatment to remove iodine.

This quarter additional data were obtained pertinent to the use of N_2O_3 sparging for removing iodine from nitric acid. Extraction and sorption tests with a variety of agents were made in an attempt to characterize the chemical behavior of the residual iodine in solution after distillation.

6.2 Iodine Control (Task 6.2)

(G. I. Cathers, J. M. Schmitt, and C. J. Shipman)

Prior studies have demonstrated that ^{131}I can be volatilized nearly completely from 4 M HNO_3 under the proper conditions. With ^{131}I -traced I_2 at an initial concentration of about 2.5×10^{-4} M, distillation of 10 to 20% of the solution usually removes 95 to 98% of the iodine. Sparging with N_2O_3 at near boiling temperatures is more effective, increasing the amount removed to 99-99.8%. Further removal is difficult even with addition of carrier iodine to isotopically dilute the residual ^{131}I because of the lack of isotopic exchange. The most promising treatment found for achieving isotopic exchange and decreasing the ^{131}I concentration to about 0.01% of its original concentration involved two cycles of (1) adding iodine carrier, (2) oxidizing the solution with ozone, and (3) sparging with N_2O_3 .

Some tests were made to determine if the N_2O_3 sparging could be carried out in a continuous manner using a countercurrent column. This would perhaps be preferred over a batch procedure in engineering practice. Results of the tests were not completely conclusive but did seem to indicate that the continuous method is feasible. The tests were made in a 1-in.-diam column that was packed with 2 ft of packing (Fig. 6-1). The liquid flow rate was 20 ml/min and the temperature was regulated to give a distillate rate of about 2 ml/min (10% cut). In the first test, which was run over a 2-hr period, the concentration of iodine in the effluent was 0.4% of that in the feed solution (Table 6-1). This is comparable to past results in batch sparging tests. Carrier iodine was added (as KI) to the column effluent to restore the iodine concentration to its original value and part of the solution was ozonized and then run through the column again (test 244B). This decreased the residual iodine to 0.14%. A second treatment of solution that had not been ozonized (244C) did not result in significant ^{131}I stripping. In a second test series, the N_2O_3 flow rate was varied from 20 to 60 ml/min. At 20 ml/min, the residual ^{131}I in the effluent was 1.6% or about a factor of 4 higher than in the earlier test with this flow rate. Increasing the N_2O_3 flow to 60 ml/min decreased the residual ^{131}I to 1.0%. Temperature regulation in these runs was not very satisfactory and trouble at times was experienced with solid iodine plugging the vapor line over the condenser. Analyses of the distillate and stripped liquid for nitrite gave values of 0.05 and 0.025 M, respectively.

ORNL DWG. 73-1925

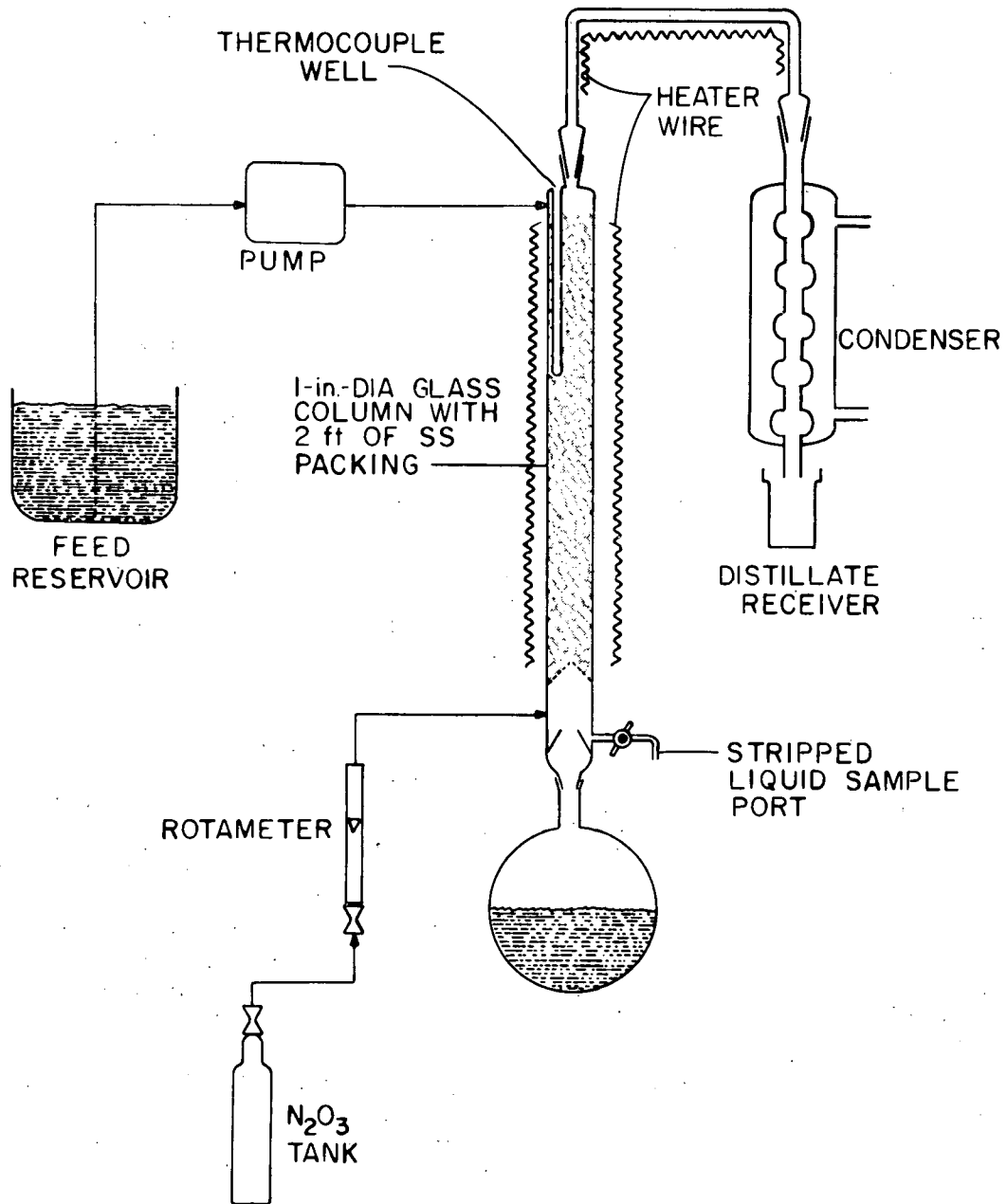


Fig. 6-1. Equipment Used in Countercurrent Stripping of Iodine from Nitric Acid.

Table 6-1. Continuous Stripping of Iodine from 4 M HNO₃ by N₂O₃ Gas in Countercurrent Column

Conditions: 20 ml/min of 4 M HNO₃ with 2.5 x 10⁻⁴ M I₂ (¹³¹I-traced) was passed through a packed column countercurrent to N₂O₃ gas (Fig. 6-1); temperature of column was adjusted to give a distillate rate of 2 ml/min; 0.5-hr to 2-hr runs.

Run No.	N ₂ O ₃ Flow (ml/min)	Residual Iodine in Column Effluent ^a (% of original ¹³¹ I)
244A	20	0.4
244B	20	0.14 ^b
244C	20	0.37 ^c
245A	20	1.6
245B	40	1.1
245C	60	1.0

^aAverage iodine level in the effluent; deviations during the run were usually in the range of ±15%.

^bSome of column effluent from run 244A was adjusted to 2.5 x 10⁻⁴ M I₂ (by addition of KI) and solution was ozonated for 20 min at 70°C before being repassed through the column.

^cSame as footnote b except solution was not ozonated.

Extraction Tests. — The above and previous studies have shown that, although most of the iodine can be distilled readily (as I₂) from dilute nitric acid, a small fraction remains which is essentially nonvolatile and obviously in a form other than elemental iodine. We recently made some extraction tests with a variety of solvents on a nitric acid solution after the distillation treatment in an attempt to characterize the chemical behavior of the residual iodine in the solution.

The 4 M HNO₃ solution, which initially contained 2.5 x 10⁻⁴ M I₂, was distilled at boiling temperature to remove 30% of the solution volume; this removed 98% of the iodine. Aliquots of this solution were contacted twice with the organic solvents, each time at a 1/1 phase ratio. The amount of iodine extracted in the two contacts ranged from about 18-19% for aliphatic diluents such as n-dodecane and n-octane to about 45% for aromatic diluents

(diethylbenzene, toluene) to 86% for hexone (Table 6-2). Extractions by a series of amine extractants and by organophosphorous esters such as TBP were in the range of 50 to 70%. Tests were made with two macroreticular resin sorbents, XAD-4 and XAD-12. These materials sorbed about 75% of the iodine. Removal of iodine from the solution by a MnO_2 strike also was investigated using a procedure being employed in studies at Savannah River;¹ this treatment removed 55% of the iodine in 20 min and 67% in 5 hr.

We have not been able to derive positive conclusions from the data of Table 6-2. Prior studies have indicated that most of the residual iodine in the solution after distillation may be in the form of organic iodides derived from impurities in the distilled water or reagents used. These organic iodides could vary greatly in molecular weight; also, some might have functional groups that would increase their hydrophilic nature and decrease their extractability. In addition, a certain fraction of the iodine could be inorganic in form such as a metal complex or iodine monochloride. The latter is known to iodinate organic materials (some more readily than others) and its presence could possibly explain some of the differences observed with the various diluents.

Because extractions with hexone were much more efficient than with other solvents, additional experiments were performed to investigate the reactions involved. Conceivably the larger extraction with hexone may indicate that the hexone undergoes the iodoform reaction typical of compounds containing the acetyl group. Normally this reaction is performed under alkaline conditions but the unique behavior of hexone with iodine in nitric acid solution suggests that the reaction possibly occurs also in 4 M HNO_3 . This reaction was of interest to us, not only as a means of understanding the chemistry of iodine in nitric acid, but also because exploitation of the reaction might allow more efficient removal of iodine from the dissolver solution.

The results of two series of ^{131}I tracer tests, with and without carrier iodine, are summarized in Table 6-3. Comparison of tests 1A and 1B show that equally good extraction was achieved either with or without carrier. This was a surprising result, but was generally confirmed by other tests in both series. In series A the initial I_2 concentration of 2.5×10^{-4} was decreased to less than 10^{-6} M by distilling 10% of the solution before extraction; reintroduction of carrier (tests 2A and 4A) had no appreciable effect on the extraction results. However, ozonation after the carrier addition (tests 3A and 5A) greatly decreased extractions apparently due to the formation of inextractable HIO_3 and HIO_4 . The addition of NO_2^- at 20°C in these two tests was not effective in reducing the iodine to the extractable form; a hot nitrite treatment after ozonation was necessary to obtain good extraction results (test 7A). In the B series of tests (without carrier) the extraction efficiency was improved by using longer contact times (tests 1B, 5B, 7B, and 9B) or a higher temperature (test 8B). Use of 5% hexone in dodecane (test 6B) gave about the same extraction as dodecane alone (test 4B).

Reference for Section 6

1. Personal communication, D. J. Crouse with Jim Kelly of Savannah River, April 1972.

Table 6-2. Extraction and Sorption of Residual Iodine from Nitric Acid After Distillation Treatment

Procedure: 4 M HNO₃--2.5 x 10⁻⁴ M I₂ solution given nitrite treatment and distilled until residual iodine was ~2% of original concentration, i.e., ~5 x 10⁻⁶ M I₂. Aliquots of solution were extracted twice, each time at a 1/1 phase ratio for 10 min.

Organic Solvent or Sorbent	Amount Extracted (%)		
	First Contact	Second Contact	Total
0.1 M Primene JM (primary amine) in DEB ^a	40.4	10.1	50.5
0.1 M Amberlite IA-1 (secondary amine) in DEB	44.3	10.5	54.8
0.1 M Adogen 364 (tertiary amine) in DEB	49.3	10.5	59.8
0.1 M Adogen 464 (quaternary) in DEB	57.9	11.5	69.4
0.5 M TBP in NDD ^b	50.4	11.5	61.9
0.5 M Diamylamylphosphonate in NDD	46.8	19.8	66.6
0.2 M Trioctylphosphine oxide in NDD	33.7	12.1	45.8
0.2 M Di(2-ethylhexyl)phosphoric acid in NDD	21.2	7.1	28.3
0.2 M Di(<u>n</u> -naphthalene)sulfonic acid in NDD	41.8	13.1	54.9
NDD	13.3	3.9	17.2
NDD + 3% tridecanol	20.8	12.2	33.0
<u>n</u> -Octane	15.1 ^c	4.4 ^c	19.5
DEB	33.6	9.5	43.1
Toluene	37.9 ^c	8.6 ^c	46.5
Hexone	76.8	8.9	85.7
1-Dodecene	23.4 ^c	5.6 ^c	29.0
XAD-12 macroreticular resin ^d	58.2	19.1	77.3
XAD-4 macroreticular resin ^d	57.5	17.8	75.3
MnO ₂ strike (~0.1 M MnO ₂)--55% removal in 20 min, 67% in 5 hr			

^a Diethylbenzene

^b n-Dodecane

^c 30-min contact

^d 1 g of resin per 10 ml of solution; 10-min contact

Table 6-3. Extraction of Iodine from 4 M HNO₃ with Hexone

Series A tests: Solution initially containing $2.5 \times 10^{-4} M I_2$ (traced with ¹³¹I) was sparged at 105°C with 300 ml/min N₂O₃ to distill 10% of the solution; the residual solution which contained only 0.24% of the original iodine, was extracted with hexone.

Series B tests: Solution containing only ¹³¹I tracer (no carrier) was treated with 0.05 M NaNO₂ for 30 min at 90°C under pressure and then air sparged to remove NO_x at 25°C; this left 41% of the original ¹³¹I (approximately $7 \times 10^{-12} M I_2$) in the solution which was extracted with hexone.

Extractions with hexone were for 10 min at 25°C and at a phase ratio of 1/1; second and third extractions with fresh hexone were made in some tests.

Test	Description	¹³¹ I Extracted (accumulative, % of original)		
		First Contact	Second Contact	Third Contact
1A	Extraction of solution A	79	84	-
2A	Added $2.5 \times 10^{-4} M I_2$ and 0.05 M NaNO ₂ before extractions	78	85	-
3A	Same as 2A except solution was ozonated after carrier addition and before NaNO ₂ addition	0.4	16	-
4A	Same as 2A except $2.5 \times 10^{-6} M I_2$ was used	78	84	-
5A	Same as 3A except $2.5 \times 10^{-6} M I_2$ was used	3.2	11	-
6A	Same as 1A except 0.05 M NaNO ₂ was used	83	85	-
7A	Same as 3A except solution was heated 30 min at 90°C after NaNO ₂ addition	85	91	-
1B	Extraction of solution B	80	88	-
2B	Same as 1B except 0.05 M NaNO ₂ added and held at 90°C for 30 min	96	97	-
3B	Solution B ozonated and then given hot NaNO ₂ treatment	85	96	-
4B	Same as 1B except solvent was dodecane instead of hexone	59	63	-
5B	Same as 1B except extraction contact time was 20 min	86	98	-
6B	Same as 1B except solvent was 95% dodecane--5% hexone	55	64	-
7B	Same as 1B except extraction contact time was 30 min	88	98.4	99.4
8B	Same as 7B except extractions were at 80°C	98	99.6	99.8
9B	Same as 1B except extraction contact time was 24 hr	95	-	-

7. SOLVENT EXTRACTION (TASK 7)
(D. J. Crouse and C. D. Watson)

The objective of Task 7 is to establish that LMFBF fuels can be processed successfully by solvent extraction methods.

Work on Task 7 has been suspended for FY 1973.

8. PLUTONIUM PURIFICATION (TASK 8)
(D. J. Crouse)

This task covers the process steps in purifying plutonium, starting with the plutonium product solution from the first Purex cycle and continuing through preparation of a product solution of adequate purity and concentration for delivery to the fuel refabrication operation.

Work on Task 8 has been suspended for FY 1973.

9. WASTE TREATMENT AND STORAGE (TASK 9)

Progress on this task is reported separately.

10. OFF-GAS TREATMENT (TASK 10)
(D. J. Crouse, O. O. Yarbrow, and C. D. Watson)

Retention of iodine will be the major problem in treating the off-gas from processing of short-cooled LMFBF fuels since plant retention factors of 10^7 to 10^8 will be required. Retention of most of the xenon, krypton, and tritium also may be required for future processing plants. All promising off-gas treatment methods will be evaluated and additional chemical and engineering data developed where necessary.

This quarter, life tests of solid sorbents were concluded after about 10 months of operation. The silver-containing sorbers maintained high efficiencies for trapping methyl iodide and I_2 over this period. A large number of runs were made in packed and bubble-cap columns to determine efficiency of the Iodex and mercury scrubbing processes for trapping iodine species over a range of conditions.

10.1 Iodine (Task 10.1)

Effect of Exposure to Simulated Off-Gas on Service Life of Sorbents
(R. D. Ackley and W. H. Hinds)

Investigation of the effects of long-term exposure to simulated fuel reprocessing off-gas on the radioiodine trapping performance of various sorbents was continued. Previous results and experimental details have been presented in our monthly reports beginning with No. 29 (July 1971).

Another set of ^{125}I -labeled elemental iodine decontamination factors was obtained, corresponding to 64 days of additional exposure; the results, together with those of the preceding set,¹ are presented in Table 10-1. (The ^{130}I -labeled methyl iodide decontamination factors usually obtained in conjunction with those for elemental iodine were not obtained this time since the information provided by previous results was deemed adequate for present purposes.) As may be noted in Table 10-1, the I_2 decontamination factors for certain of the test situations corresponding to 350 days of exposure are indicative of some reduction in capability for trapping and retaining iodine injected as I_2 . However, even the lowest of these decontamination factors, 5×10^2 , is satisfactorily high.

The life tests are being concluded and a topical report is being prepared covering our studies (including the life tests) of solid iodine sorbents.

Iodex Process: Scrubbing I_2 from Air in a Six-Stage Bubble-Cap Column With Concentrated Nitric Acid (G. I. Cathers and W. E. Shockley)

Previously work was reported on the decontamination of air containing ^{131}I -traced methyl iodide in a 1-in.-diam simulated bubble-cap column. The results of 22 runs with air containing ^{131}I -traced I_2 vapor are presented in this report. This work has generally confirmed that higher decontamination is obtained for I_2 than for CH_3I , due probably to the slower reaction rate for decomposition of CH_3I to I_2 before the latter can be converted to iodic acid in the concentrated nitric acid.

A schematic diagram of the improved equipment used near the end of the series of 22 runs is shown in Fig. 10-1. At the beginning of the series, the equipment was somewhat different with changes being made as the runs proceeded; these changes are described in the data tables. The major changes in the column involved variation of the liquid level or inventory in each bubble-cap stage. Originally, a caustic countercurrent packed column followed the bubble-cap column; this was eliminated later and a larger condenser with ice-water cooling was used for effective trapping of nitric acid fumes.

Free iodine (traced with ^{131}I) was prepared for these tests by mixing KI with ^{131}I tracer in 0.01 M NaHSO_3 solution, adding this solution to 4-6 M HNO_3 solution to form and precipitate I_2 crystals, and filtering and washing the I_2 on a frit filter. Water was removed by evacuation to below

Table 10-1. Elemental Iodine Decontamination Factors for Sorbents Exposed to Simulated LMFBR Fuel Reprocessing Off-Gas

Sorbent ^a	Form of Sorbent	Temp. (°C)	Hopcalite Upstream?	Preceding Results		Recent Results	
				Exposure Time (days)	DF ^b	Exposure Time (days)	DF ^c
25% silver zeolite	1/16-in. pellets	200	No	286	4 x 10 ⁴	350	8 x 10 ³
			Yes	286	1 x 10 ⁴	350	3 x 10 ³
88% silver zeolite	10 x 20 mesh beds	200	No	90	>1 x 10 ⁵	154	>1 x 10 ⁴
			Yes	90	>1 x 10 ⁵	154	>1 x 10 ⁴
99% silver zeolite	1/16-in. pellets	100	No	195	>1 x 10 ⁵	259	>1 x 10 ⁴
			Yes	195	>1 x 10 ⁵	259	>1 x 10 ⁴
GX135 (silver salt-treated alumina-silica)	8 x 16 mesh granules	100	No	209	>1 x 10 ⁵	273	>1 x 10 ⁴
			Yes	90	2 x 10 ⁴	154	>1 x 10 ⁴
GX135		200	No	286	2 x 10 ⁴	350	5 x 10 ²
			Yes	286	>1 x 10 ⁵	350	>1 x 10 ⁴

^aSorbent depths are 2 in.

^bEach of these values is based on the calculated amount of ¹²⁵I entering the test bed section and the observed amount of ¹²⁵I penetrating to the collection bed section during the last 61 days of the indicated exposure period.

^cAs the preceding except for the time period which was 64 days. (Also, counting level was somewhat lower.)

ORNL DWG. 73-770

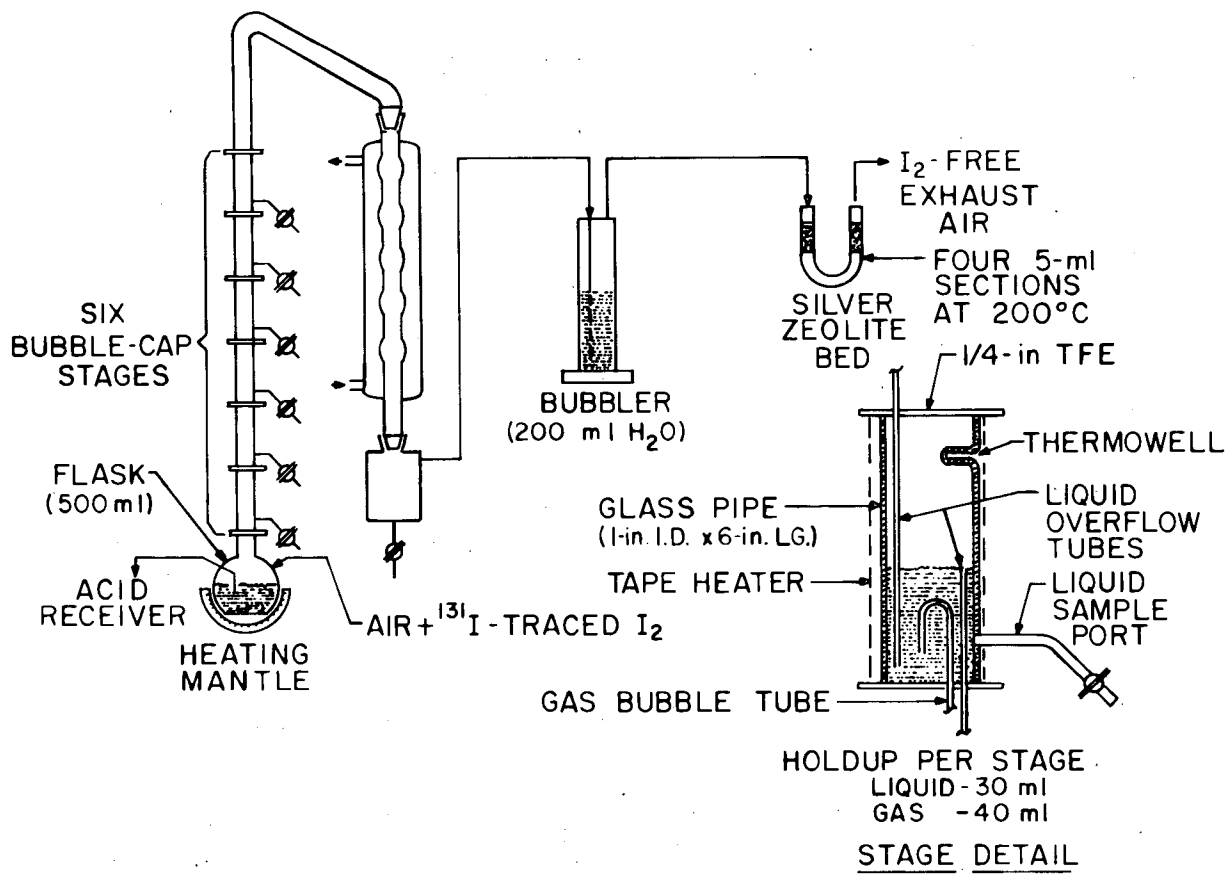


Fig. 10-1. Six-Stage Simulated Bubble-Cap Column and Associated Equipment.

the vapor pressure of water but not below the vapor pressure of I_2 (0.3 mm at 25°C). The dry iodine on the filter frit was vaporized at 50°C with 50 cc/min of air which was then mixed with the main stream of air that was fed to the scrubbing column.

The first series of runs summarized in Table 10-2 was designed primarily to study the effect of liquid flow rate and temperature at an air flow rate of 1.6 liters/min; one run was made at 2.5 liters/min. All of the measured stage DF's were at least twice as large as those measured for CH_3I previously. Runs 8, 9, and 10 at 25, 50, and 75°C, respectively, confirmed other work indicating that the optimum temperature for scrubbing with 18 M HNO_3 is about 50°C. However, the difference in the average stage DF's for these runs was small. Increasing the 18 M HNO_3 flow rate from 10 ml/min (run 9) to 18 ml/min (run 11) increased the average stage DF by about 20%. At the 18 ml/min liquid flow rate, increasing the gas flow from 1.6 to 2.5 liters/min decreased the average stage DF by about 15%.

In a perfectly mixed system, the stage decontamination factor is related to the I_2 partition coefficient, H , and the reaction rate constant, λ , as follows:

$$DF - 1 = \frac{HL}{G} + \frac{HV\lambda}{G}, \quad (1)$$

where G and L are the gas and liquid flow rates, and V is the liquid inventory per stage. We are trying to evaluate the important parameters, H and λ , by operating the scrub column at various liquid and gas flow rates and observing the change in decontamination factor. In the runs reported in Table 10-2, however, the reproducibility of results for duplicate runs (runs 9 vs 15, runs 13 vs 14) was not good. We think that the nitrite concentration of the acid used in runs 11-15 was lower than that of acid used in runs 8-10 which may explain the higher efficiencies obtained in the later runs. In subsequent work, a special effort was made to use nitric acid with a nitrite content of less than 10^{-4} M. This was done with air sparging or ozone treatment to make the acid colorless, a treatment found by analysis to be adequate.

The second series of runs (Table 10-3) was designed to study the effect of liquid flow rate and the presence of special oxidizing agents dissolved in the nitric acid. Two changes were made in the system: one was a change in the liquid overflow weir tubes to make the liquid inventory per stage about 10 ml instead of 30 ml; the second change involved installation of a slot-type gas dispersal tube in each stage. These two changes increased the gas throughput that can be obtained without flooding, i.e., forcing of liquid from one stage into the next higher stage. Tests with water showed that flooding did not occur even at a gas flow rate of 12 liters/min.

The effect of varying the 18 M HNO_3 flow from 5 to 18 ml/min was studied in the first three runs at 50°C. As expected, the DF increased with liquid flow rate (Table 10-3). At the risk of placing too much emphasis on three results, equation (1) for the DF per stage is tested

Table 10-2. Results of Six-Stage Bubble-Cap Column Tests on Scrubbing I₂ from Air with 18 M HNO₃

Procedure: System consisted of bubble-cap column followed by a water-cooled condenser, a packed column with circulating 1 M NaOH solution^a and a 200°C silver zeolite bed. Bubble-cap stages had 30-ml liquid holdup (3-in.-length) with the gas being introduced near bottom of each stage through a simple submerged tube (2.5-in.-depth). Runs were for 2 hr with air containing 50-100 ppm I₂; acid was not recycled.

	8	9	10	11 ^a	12	13	14	15
Temperature (°C)	25	50	75	50	50	50	50	50
Gas flow rate (liters/min)	1.6	1.6	1.6	1.6	2.5	1.6	1.6	1.6
Liquid flow rate (ml/min)	10	10	10	18	18	13.3	13.3	10
DF across the bubble-cap column	4.4x10 ³	9.8x10 ³	4.9x10 ³	3.0x10 ⁴	6.1x10 ³	4.0x10 ⁴	6.6x10 ⁴	5.4x10 ⁴
DF across condenser	-	22	4.9	36	330	62	25	77
DF across the total system ^b	5.0x10 ³	2.2x10 ⁵	6.9x10 ⁴	1.1x10 ⁵	2.0x10 ⁵	2.5x10 ⁵	1.7x10 ⁵	4.2x10 ⁵
Individual stage DF - Stage 6	5.63	6.17	7.09	11.7	8.76	4.57	14.8	12.0
- Stage 5	4.73	3.80	3.73	3.70	3.64	14.8	4.99	5.78
- Stage 4	4.37	5.10	4.09	5.51	4.80	5.46	6.22	5.90
- Stage 3	4.15	4.67	4.12	5.51	4.28	5.60	5.91	6.05
- Stage 2	3.97	4.75	3.79	5.65	3.85	5.32	5.47	5.41
- Stage 1	3.49	4.08	3.28	4.83	3.48	4.77	5.10	5.10
Average stage DF ^c	4.05	4.63	4.12	5.58	4.80	5.85	6.37	6.15

^aIn run 11 and subsequent runs, a simple water bubbler was used in place of the caustic scrub column.

^bTotal DF across scrub column, water-cooled condenser, and caustic or water scrub; essentially all of the DF beyond that obtained in the scrub column was obtained in the condenser.

^cAverage stage DF = $\sqrt{\text{column DF}}$.

Table 10-3. Results of Six-Stage Bubble-Cap Column Tests on Scrubbing I₂ from Air with 18 M HNO₃ or with 18 M HNO₃ Containing Oxidizing Agents

Procedure: System same as shown in Fig. 10-1 except that bubble-cap stage inventory was changed from 30 to 10 ml and a slotted gas dispersion tube was used (1-in.-depth of immersion in 1 in. of liquid).

Run No.	16	17	18	19	20
Temperature, °C	50	50	50	50	50
Gas flow rate, liters/min	1.6	1.6	1.6	1.6	1.6
Liquid flow rate, ml/min	10	18	5	5	5
Oxidizing agent and concentration, M	-	-	-	0.005 KMnO ₄	0.008 K ₂ CrO ₄
DF across bubble-cap column	4010	6680	1540	3220	4510
DF across condenser	3.7	6.8	5.8	6.9	5.4
DF across total system ^a	1.13 x 10 ⁵	1.34 x 10 ⁵	1.15 x 10 ⁵	1.97 x 10 ⁵	1.89 x 10 ⁵
Individual stage DF - Stage 6	9.50	8.12	8.05	17.8	12.4
5	4.50	4.57	3.88	4.06	4.05
4	4.57	4.97	3.54	3.56	3.59
3	4.01	4.07	3.03	2.91	3.43
2	3.07	3.35	2.36	2.29	2.56
1	3.25	3.53	2.50	2.37	3.57
Average stage DF ^b	3.99	4.34	3.40	3.84	4.07

^aExclusive of the silver zeolite trap.

^bAverage stage DF = $\sqrt[6]{\text{column DF}}$.

in Fig. 10-2. From the slope of the linear relationship assumed, the partition coefficient, H , was calculated to be 115; the intercept at zero flow rate gives a λ value of 0.18 sec^{-1} or a reaction half-time of 3.8 sec. These values are reasonably close to those expected, but additional data must be obtained over a wider range of conditions before reliance can be placed on this correlation. It is of interest to compare this reaction constant of 0.18 sec^{-1} at 50°C to that obtained at 25°C in spectrophotometric studies (see next section) where a half-time value of 12.5 sec^{-1} was obtained; the latter value is equivalent to a reaction constant of 0.055. The 3.3-fold difference between the two values is roughly what would be expected for a 25°C temperature difference. Table 10-3 also shows the favorable effect obtained with use of KMnO_4 or K_2CrO_4 in the nitric acid (compare runs 19 and 20 with run 18). The beneficial effect of the oxidizing agents can probably be attributed, at least partly, to the fact that they would rapidly destroy any nitrite in the solution.

Table 10-4 presents data obtained in runs designed to determine the effect of gas flow rate on the decontamination efficiency. The gas flow rate was varied from 1.6 to 6.4 liters/min; the liquid holdup was 10 ml per stage. The 4.8- to 6.4-liter/min. range is more realistic than 1.6 liters/min for engineering application. The values for various runs of $G(\text{DF} - 1)$, which is derived from equation (1) are shown in Table 10-5 to be approximately constant, i.e., $\text{DF} - 1$ is about inversely proportional to the gas flow rate. In run 27 the liquid holdup was changed from 10 ml/stage back to 30 ml/stage while retaining use of the slotted tube for gas dispersion. The slotted tube, however, was submerged only 1 in. instead of 3 in. as in the earlier runs (Table 10-2) with 30-ml holdup. Surprisingly, results in runs 27, 30, and 31 with the 30-ml liquid inventory were slightly poorer than the corresponding runs with 10-ml inventory. This was probably because the gas inlet tube was submerged only 1 in., leaving a stagnant liquid depth of about 2 in. in the test at 1.6 liters/min. At 4.8 liters/min, there was better liquid agitation below the dispersion point so that run 31 compares favorably with run 23.

Table 10-5. Test of the Constancy of the Product $G(\text{DF} - 1)$ in Runs 21-24

Run No.	G (liters/min)	DF	$G(\text{DF} - 1)$
21	1.6	4.35	5.4
22	3.2	3.38	7.6
23	4.8	2.37	6.6
24	6.4	1.80	<u>5.1</u>
		Average	6.2

ORNL DWG 72-13886 R1

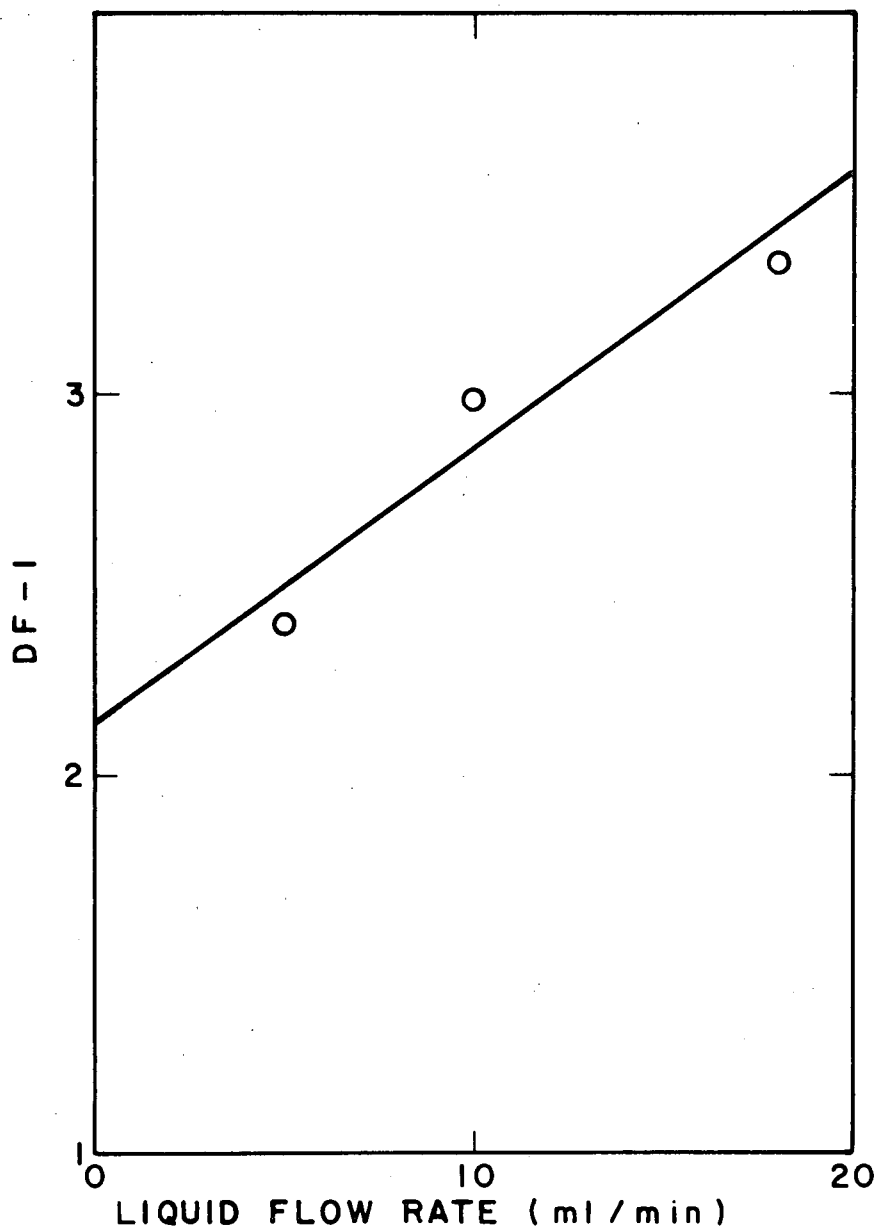


Fig. 10-2. Correlation of the Bubble-Cap Stage DF with Liquid Flow Rate.

Table 10-4. Results of Six-Stage Bubble-Cap Column Tests on Scrubbing I₂
From Air with Concentrated HNO₃ at 50°C

Procedure: System as shown in Fig. 10-1; liquid flow rate was 10 ml/min; liquid inventory was changed from 10 ml/stage (runs 21-24) to 30 ml/stage (runs 27-31). Gas was dispersed through a slotted-glass tube at a depth of about 1 in. Condenser efficiency was improved by using 5°C cooling water in runs 23-31.

Run No.	21	22	23	24	27	28	29	30	31
HNO ₃ concentration, M	18	18	18	18	18	19	19	18	18
Gas flow rate, liters/min	1.6	3.2	4.8	6.4	1.6	1.6	4.8	1.6	4.8
DF across bubble-cap system	6800	443	177	33.5	2440	8.6x10 ⁴	1030	3800	125
DF across condenser	36	15	51	24	150	5.6	179	33	1080
DF across entire system ^a	7.0x10 ⁵	1.8x10 ⁵	3.5x10 ⁴	2490	3.7x10 ⁵	4.8x10 ⁵	1.8x10 ⁵	2.7x10 ⁶	2.6x10 ⁵
Individual stage DF									
Stage 6	8.52	1.18	2.80	1.85	3.38	1	3.94	4.16	2.58
Stage 5	4.24	3.77	2.63	2.14	3.59	64	3.15	3.74	2.32
Stage 4	4.67	3.31	2.73	1.96	4.02	8.35	2.98	4.56	1.99
Stage 3	5.00	3.16	2.39	1.91	4.20	8.91	3.75	4.19	2.33
Stage 2	3.26	2.18	1.89	1.59	2.60	4.98	2.64	3.20	1.91
Stage 1	3.79	2.48	2.03	1.51	3.81	5.81	2.85	3.42	2.16
Average stage DF ^b	4.35(6)	3.38(5)	2.37(6)	1.80(6)	3.67(6)	6.81(4)	3.18(6)	3.95(6)	2.23(6)

^aTotal DF across the bubble-cap column, condenser, and water bubbler.

^bAverage stage DF = $\sqrt[x]{\text{column DF}}$, where x was the number of stages in which the DF was significantly >1. In run 28, the average was calculated as the geometric mean of the DF's for the lower four stages; x is designated in parentheses.

Two runs were made with 19 M HNO_3 at 1.6 and 4.8 liters/min air flow. These runs (28 and 29) demonstrated the large favorable effect of increasing the acid concentration (compare to runs 21 and 23). Increased attention will be given in future work to concentrations higher than 18 M. This should increase the efficiency when using a bubble-cap tower for scrubbing organic iodides.

The effect of higher acid concentration is seen also in the large DF's quite often obtained in the condenser used for trapping the nitric acid fumes from the column. Generally the condenser DF was higher when the column DF was low and there was considerable I_2 reaching the condenser. The condenser effect varies also with column temperature and air flow rate. In the 2-hr runs, the amount of condensate that was collected varied from 14 to 34 ml, being better in later runs where a larger condenser was installed and 5°C cooling water was used. The amount of condensate was roughly proportional to the gas flow rate, being, for example, 88 ml at 6.4 liters/min. Higher condenser DF's were obtained with the larger amounts of condensate. The molarity of the condensate in 18 M HNO_3 runs was generally 21.1 to 21.7 M. In using 19 M HNO_3 , the condensate was 22.8 M.

We are modifying the column and will explore further the optimum conditions of acid concentration and temperature with air- I_2 mixtures. Following this, additional runs will be made in the column with methyl iodide in the air stream.

Spectrophotometric Study of the Reactions of Iodine in Concentrated Nitric Acid Solutions. (G. I. Cathers and A. H. Kibbey)

Spectrophotometric studies of the iodine-nitric acid system,² using a Cary-14 spectrophotometer, were continued in an effort to determine reaction rates for I_2 oxidation to iodic acid as a function of nitric acid and nitrite ion concentrations.

In our latest series of runs, ~18 M HNO_3 was made 5×10^{-4} M in I_2 (added as NaI which converts to I_2 quickly), and the reaction subsequently quenched after 5, 10, or 20 sec by dumping in 2 parts of 4°C ice water to lower the acid concentration to ~6 M. Reference solutions without I_2 for the spectrophotometer were prepared with 5×10^{-4} M NaNO_2 in simulation of the NO_2^- ion produced by the oxidation of I^- to I^0 . The diluted solutions, in 10.0 cm cells, were periodically scanned between 4000 Å and 6000 Å; the rise in height of the I_2 peak occurring in the vicinity of 4700 Å was indicative of the reduction to I_2 of the IO_3^- initially formed in the strong acid. By plotting the increasing I_2 absorbance peak (Fig. 10-3) against time-after-quench, and then extrapolating back to $t = 0$, the relative amount of I_2 present in the concentrated HNO_3 solution at quench time was estimated. The absorbance data obtained at zero observation time in the spectrophotometer with the 6 M HNO_3 solutions were compared to the absorbance of a special 6 M HNO_3 solution containing one-third the I_2 concentration of 5×10^{-4} M used in the 18 M HNO_3 solution. This allowed calculation of the percentage of unreacted I_2 as a function of reaction time, as shown in Fig. 10-4.

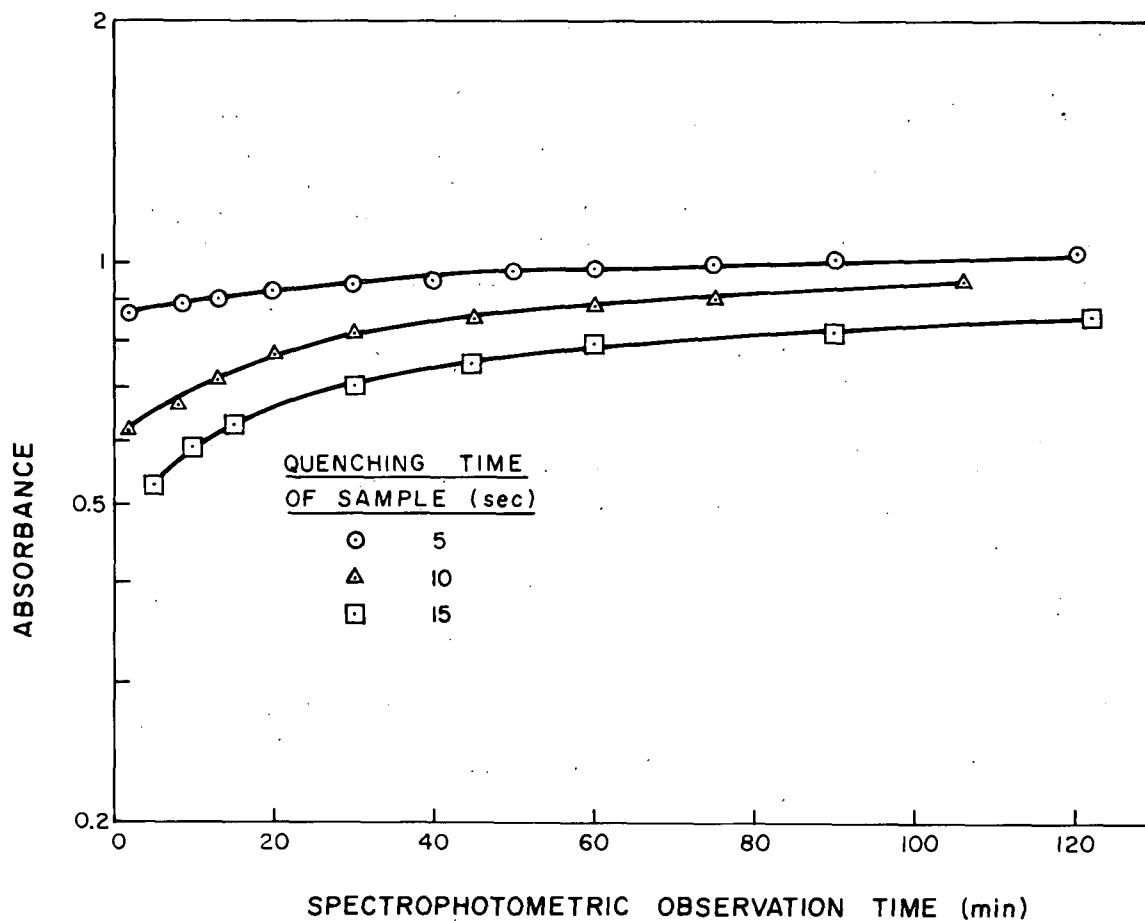


Fig. 10-3. Rate of Increase of I_2 Concentration in Nitric Acid Solution After Dilution from 18 M to 6 M (Increase is Attributed to Iodic Acid Reduction to I_2 by Nitrous Acid Present in the Solution). Samples that were obtained by quenching the reaction of I_2 with 18 M HNO_3 were observed spectrophotometrically for about 2 hr after quenching. Test solution: 17.7 M HNO_3 , initially 5×10^{-4} M I_2 , reaction quenched by dilution to 6 M HNO_3 after 5, 10, or 15 sec. Reference solution: 17.7 M HNO_3 , 5×10^{-4} M $NaNO_3$, quenched as for test solution.

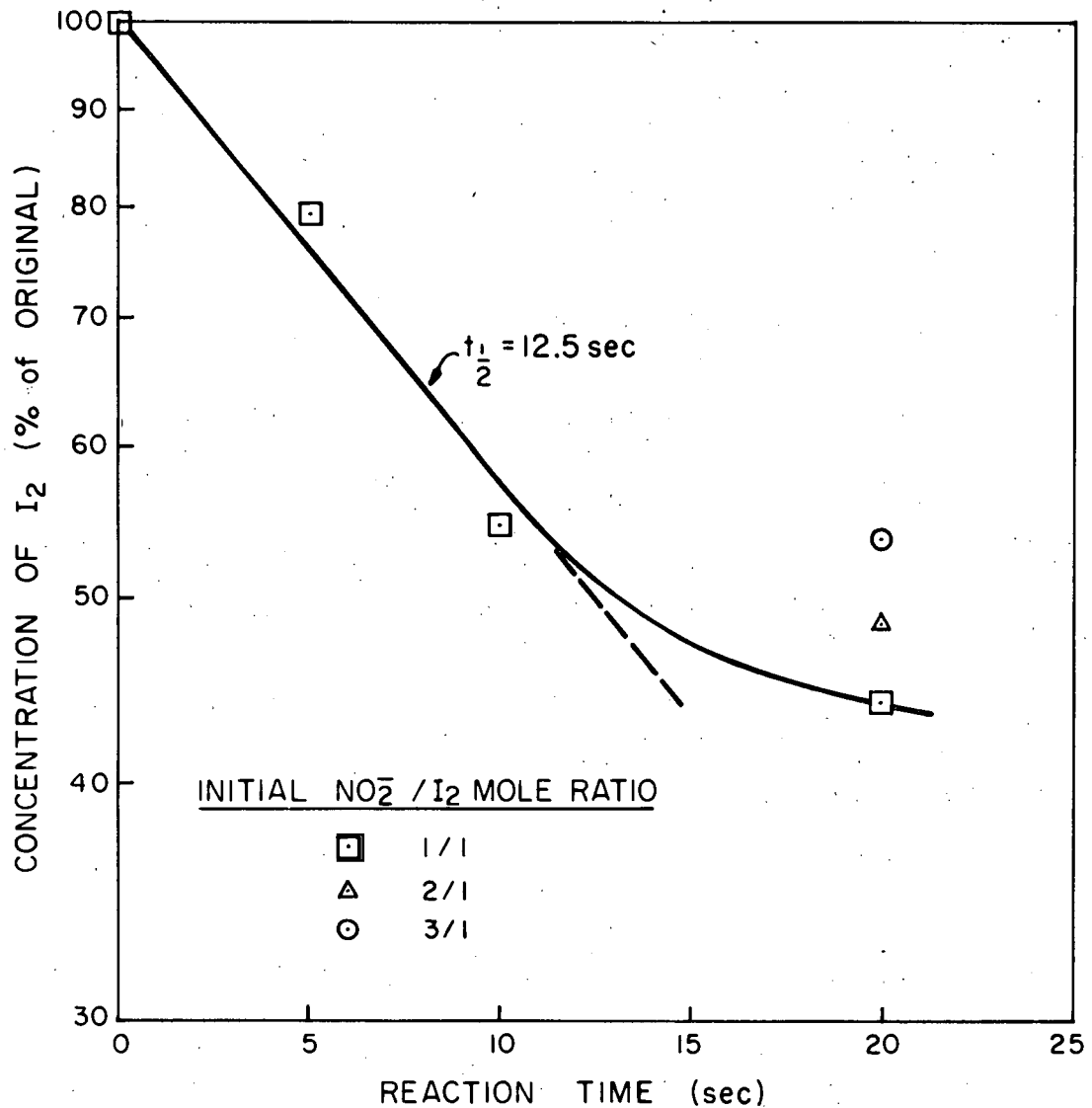


Fig. 10-4. Reaction Rate Data for Conversion of I₂ to Iodic Acid in 18 M HNO₃ at ~ 25°C. Procedure: 5 x 10⁻⁴ M I₂ added (as NaI at zero time) to 17.7-18.2 M HNO₃ that had been ozonized and air-sparged to eliminate nitrite (nitrite was added in two of the tests); reaction quenched at indicated time by addition of ice water; I₂ concentration in the solution determined spectrophotometrically.

The amounts of unreacted I_2 shown at reaction quench times of 5 and 10 sec indicate a first-order reaction with a half-time of 12.5 sec. The point at 20 sec indicates a slowing down of the I_2 to IO_3^- reaction, probably due to the increasing amount of nitrite ion accumulated by the reduction of nitric acid. The initial nitrite ion concentration at zero reaction time should have been 5×10^{-4} M, due to the essentially instantaneous oxidation of I^- to I_2 . At 20-sec reaction time, the calculated nitrite ion concentration was 1.9×10^{-3} M. The curvature shown in the plot of Fig. 10-4 probably represents an approach to an equilibrium condition. Two special runs at 20-sec quench times are shown in Fig. 10-4; in these tests $NaNO_2$ was added to the 18 M HNO_3 prior to addition of the NaI so that the nitrite concentration at essentially zero reaction time was 2 or 3 times that in the first run. The respective calculated nitrite ion concentration values at 20 sec were 2.4×10^{-4} and 2.9×10^{-4} M. As expected, increasing the nitrite ion content resulted in less I_2 oxidation.

Engineering Studies of the Iodex Process
(W. S. Groenier and D. E. Spangler)

The countercurrent scrubbing of air containing ^{131}I -tagged CH_3I , using nitric acid in a 4-cm-diam x 117-cm-long column packed with 1/4-in. beryl saddles, was continued in a run Series IX-7 through IX-12. The purposes of these studies were to gain additional verification of the methyl iodide decontamination factors (DF) that had been measured in previous experiments performed in a shorter packed column (56 cm), to measure DF values at different liquid flow rates, and to obtain DF values at temperatures intermediate to those previously used.

Most runs were made using an acid feed rate of ~ 300 cc/min and an air feed rate of ~ 3 liters/min. The acid was not recirculated, but used on a once-through basis. Condensed vapors were collected separately and not returned to the column.

Results of all of the methyl iodide runs are tabulated in Table 10-6. The DF values of runs made at similar conditions are graphed as a function of mean gas residence time in Fig. 10-5 to demonstrate a data correlation method recently adopted. The slope of each line in the figure is the correlating parameter defined in the discussion below.

In an earlier report,¹ we indicated good agreement between DF values obtained in long and short columns using 70% and 80% HNO_3 at temperatures of about $100^\circ C$. This agreement was between DF values per foot of packing per unit of mean gas residence time, and it indicates that column scale-up designs can be accomplished directly by using these DF-per-foot values. The correlating parameter $[\ln(DF)]/(\text{mean gas residence time per foot of packing, sec})$ for runs IX-1-5,9 and IX-3-1,2 (70% HNO_3 , $105^\circ C$, short column) averaged 0.74, which compares with a value of 0.99 for runs IX-7-1 and IX-11-1 (70% HNO_3 , $100^\circ C$, long column). The correlating parameter for runs IX-3-3,4,7 (80% HNO_3 , $100^\circ C$, short column) averaged 3.21, which agrees with a value of 3.01 for run IX-7-2 (80% HNO_3 , $98^\circ C$, long column). All runs were made using similar acid flow rates.

Table 10-6. Iodex Process - Removal of Methyl Iodide from Air

(Single-pass operation of a 4-cm-diam tower packed with 1/4-in. beryl saddles)

Run No.	HNO ₃ (M)	Tower Temperature (°C)	Air Flow (liters/min)	Acid Flow (ml/min)	Column Packed Length (cm)	Gas Residence Time (sec)	Decontamination Factor Over Packed Column	Correlating Parameter ^a
8-1	18.8	96	4.7	230	117	3.0	8.1 x 10 ⁴	3.80
8-2	18.8	76	4.7	250	117	5.1	(6.6 x 10 ⁵) ^b	2.62
3-4	18.1	99	4.5	290	56	0.9	17	3.22
3-3	18.1	99	3.1	280	56	1.1	24	3.03
3-6	18.1	101	3.2	280	56	1.1	(130)	(4.32)
3-7	18.4	101	3.0	240	56	1.1	48	3.39
7-2	18.6	98	3.0	250	117	3.1	1.1 x 10 ⁴	3.01
3-5	18.0	72	3.1	270	56	4.3	30	0.80
10-2	17.8	69	6.2	440	117	4.6	3.5 x 10 ⁴	2.26
10-1	18.1	72	4.7	250	117	6.7	2.5 x 10 ⁴	1.52
12-3	18.2	74	4.7	130	117	7.1	4.5 x 10 ⁴	1.51
12-1	18.4	48	3.0	250	117	11.5	4.0 x 10 ³	0.72
12-2	18.1	53	3.0	130	117	12.4	4.9 x 10 ⁴	0.87
9-1	18.2	28	6.2	410	117	5.5	2.4 x 10 ⁴	1.84
3-8	18.1	30	3.0	270	56	5.8	120	0.82
9-2	18.3	27	6.2	230	117	6.2	7.1 x 10 ⁴	1.81
3-2	15.7	104	4.5	250	56	1.2	2	0.72
3-1	15.7	105	3.0	250	56	1.5	2	0.55
1-9	14.8	106	3.4	270	56	1.7	4	0.78
1-5	15.6	104	3.3	270	56	1.7	5	0.89
1-6	15.6	104	3.3	430	56	1.8	4	0.83
11-2	15.7	97	3.0	410	117	4.7	260	1.17
11-1	15.7	97	3.0	240	117	5.0	110	0.94
7-1	15.7	102	3.0	250	117	5.5	290	1.04
1-3	15.0	94	3.1	610	56	1.6	2	0.55
1-4	15.0	92	3.1	270	56	1.9	1	0
1-2	15.0	89	3.1	260	56	2.3	1	0
1-1	15.0	82	3.1	280	56	3.3	1	0.10
1-7	15.6	79	3.4	290	56	4.3	4	0.32

^a Correlating parameter = $[\ln(\text{DF})]/(\text{gas residence time})$ on the basis of 1 ft of packing.

^b Condenser DF = 1.4, overall DF = 9.3×10^5 .

ORNL DWG 73-58

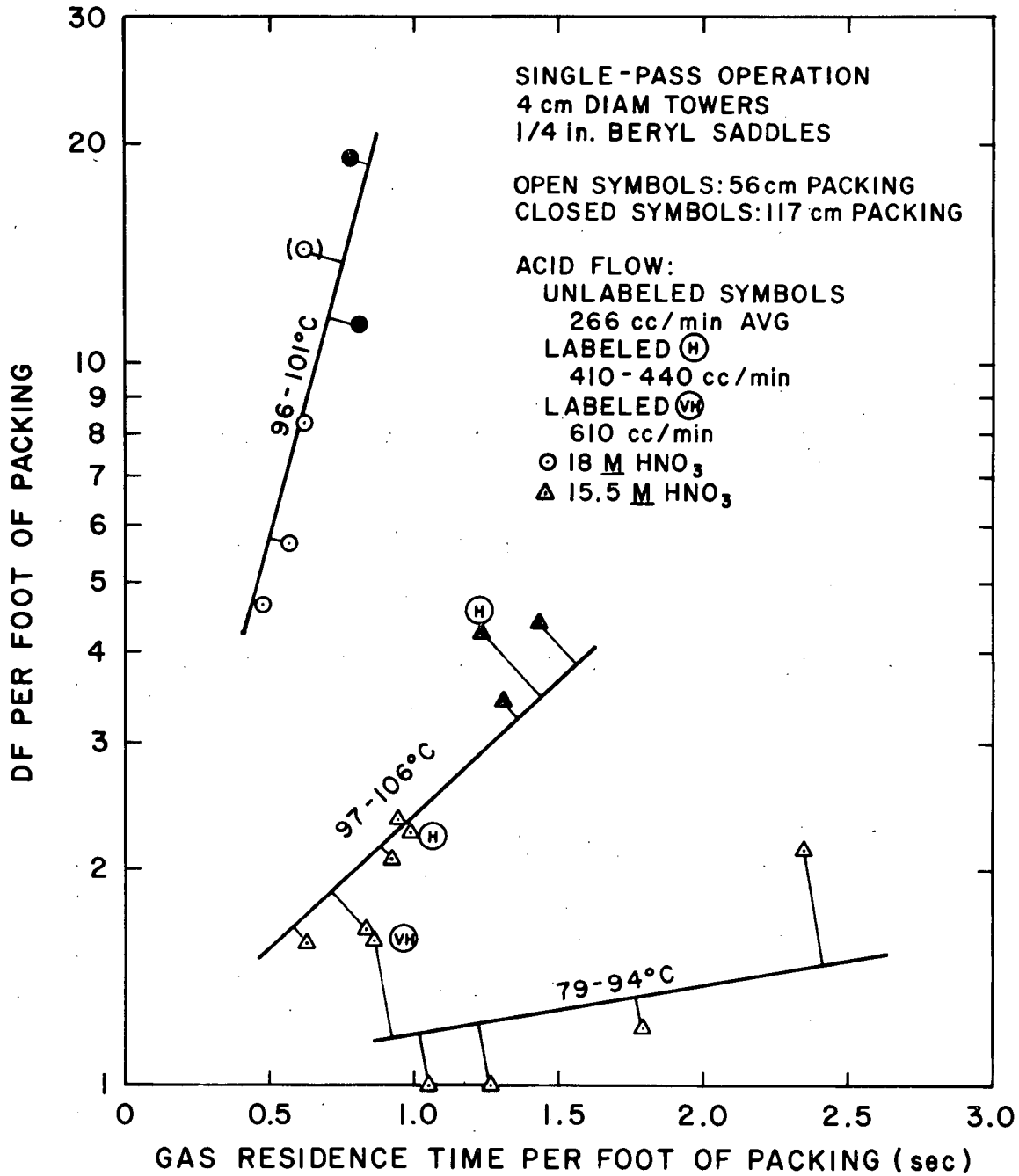


Fig. 10-5. Iodex Process - Effect of Gas Residence Time on Methyl Iodide Removal. Single-pass operation; 4-cm-diam column with 1/4-in. beryl saddles.

At lower temperatures, methyl iodide DF values per foot of packing are higher in the long column than in the short column. This seems to indicate that at the lower temperatures the methyl iodide is more difficult to destroy and more residence time for nitric acid reaction is required. Evidence for this is from run IX-3-5 (80% HNO_3 , 72°C, short column, parameter = 0.80) and run IX-10-1 (80% HNO_3 , 72°C, long column, parameter = 1.52); also from run IX-3-8 (80% HNO_3 , 30°C, short column, parameter = 0.82) and run IX-9-2 (80% HNO_3 , 27°C, long column, parameter = 1.81).

The effect of a higher liquid flow rate is to decrease the gas residence time because of a higher liquid holdup in the packing, but it also promotes more vigorous gas-liquid mixing. The net effect in three cases, where the liquid flow was nearly double that normally used, was to increase the correlating parameter. The increase was 15% in run IX-11-2 (compared to IX-11-1 and IX-7-1) and in IX-1-6 (compared to IX-1-5,9 and IX-3-1,2) where 70% HNO_3 at ~100°C was used. It was as much as 49% in run IX-10-2 (compared to IX-10-1) where 80% HNO_3 at ~70°C was used. No change was indicated in run IX-9-1 (compared to IX-9-2), which was made using 80% HNO_3 at ~30°C.

The use of a lower liquid rate (about one-half of normal) produced no significant change in the correlating parameter, as seen by comparing run IX-12-3 with IX-10-1, and run IX-12-2 with IX-12-1.

Values of the methyl iodide correlating parameter are plotted as a function of temperature in Fig. 10-6. Included are the values for Series IX-8, not previously discussed, because the unusually high acid concentration used in these runs prevented direct comparisons with other runs. Note that in run IX-8-2 we obtained the highest overall DF of nearly 10^6 . Interpolation of these results, and application to an engineering-scale design basis, results in the predicted decontamination factors per foot of column shown in Table 10-7 for two air flow rates at an 80% HNO_3 flow of about 320 gal hr^{-1} ft^{-2} .

Table 10-7. Predicted Methyl Iodide Decontamination Factors

(80% HNO_3 , 320 gal hr^{-1} ft^{-2})

Temperature (°C)	Decontamination Factor Per Foot of Packing	
	Air Flow (cfm/ ft^2)	
	7.8	15.7
30	8.5	2.9
40	11	3.4
50	17	4.2
60	27	5.3
70	43	7.1
80	55	9.3
90	51	11
100	27	11

Translated to the treatment of a 100-cfm air stream, the predictions indicate that to obtain an overall DF of 10^6 for methyl iodide using 80% HNO_3 at 60°C , a 34-in.-diam column with 99 in. of packing would be required.

Scrubbing of Iodine from Gas Streams with Mercuric Nitrate Solutions

(D. J. Crouse, J. M. Schmitt, and W. B. Howerton)

In the mercury scrubbing process, the scrub solution is circulated in closed cycle. In such a system the decontamination efficiency is controlled not only by the ability to remove iodine from the feed gas but also by the ability to retain the accumulated iodine in solution in a fixed nonvolatile form.

In earlier tests², the decontamination factors obtained on scrubbing methyl iodide from air with $0.4\text{ M Hg}(\text{NO}_3)_2$ - 8 M HNO_3 solution in a packed column (1-in.-diam, 5.5 ft of packing) were 9×10^6 and 70, respectively, for air flow rates of 2.5 and 9.5 liters/min. In these tests, the scrub solution was pumped in closed cycle from the bottom to the top of the column. The results were consistent with the assumption that the decontamination efficiency was controlled primarily by the rate of reaction of methyl iodide with mercury in the aqueous phase to form a non-volatile mercury-iodine complex. In tests with I_2 , increasing the air flow rate from 2.5 to 9.5 liters/min decreased the DF by a factor of only 8; at 2.5 liters/min, the DF for CH_3I was about a factor of 10 higher than for I_2 . Reexamination of the I_2 data and interpretation of some newer data indicate that, in the I_2 system, the absorbed I_2 is converted very rapidly to other iodine species, and the decontamination efficiency is controlled primarily by bleed-off of iodine (probably in the form of organic iodides) from the recycle solution.

In a new series of I_2 runs in the 1-in.-diam packed column, the DF when scrubbing with $0.4\text{ M Hg}(\text{NO}_3)_2$ - 8 M HNO_3 solutions at an air flow of 3 liter/min was about 4000. The results were improved by ozonating the recycle solution (to remove organic impurities) or by adding N_2O_3 to the feed air stream but the improvements were not large. In a run with an air flow rate of 7 liter/min, the DF was 973 and the ^{131}I concentration in the gas leaving the column was 7.9 counts/min per liter. At the conclusion of this run, the air flow was continued for 2 hr but with no I_2 input. The off-gas from the column contained 5.3 counts/min of ^{131}I per liter of gas over the first hour and 4.3 counts/min over the second hour, indicating that bleed-off of iodine from the solution was essentially controlling the decontamination efficiency. In one run, a second packed column (3 ft of packing) containing recirculating $0.4\text{ M Hg}(\text{NO}_3)_2$ -- 8 M HNO_3 was used in series with the first column. This increased the value of the DF by less than 50%. The iodine leaving the first column was apparently in a form that is much more difficult to trap than methyl iodide or I_2 since subsequent tests showed that the second column would have provided a DF of about 50 for methyl iodide and 3500 for I_2 under the test conditions.

Some sparging tests were then made in an attempt to obtain a better understanding of the factors affecting iodine release from the scrub

solutions. In the initial test series, solutions containing 0.01 M $\text{Hg}(\text{NO}_3)_2$ --0.2 M HNO_3 -- 6×10^{-4} M I_2 were prepared by mixing I_2 --0.2 M HNO_3 solution with 0.02 M $\text{Hg}(\text{NO}_3)_2$ --0.2 M HNO_3 solution. The solutions were then sparged with air for 2 hr. Based on the amount of iodine released during sparging, the liquid/gas iodine distribution coefficient (D_G^L) was 2.9×10^6 when ozonized water (prior studies have shown that ordinary distilled water contains organic impurities that are destroyed by an ozone treatment) was used in preparing the solution; when ordinary distilled water was used, the amount of iodine released was higher by a factor of 3. Aging the latter solution for 20 hr prior to sparging decreased the iodine release by a factor of 5 ($D_G^L = 5.3 \times 10^6$).

In a second test series, all at 0.4 M Hg^{2+} concentration, the acid concentration in the solution was varied from 1 M to 12 M. All of the D_G^L values were in the range of 8×10^6 to 2.3×10^7 , with the highest value being obtained at the highest acid concentration. Adding 0.05 M NaNO_2 to the mercury solution prior to the addition of I_2 decreased the iodine volatilized by a factor of 1.5-2.

An attempt was made to prepare a solution devoid of organic contaminants to see how this affected the results. An I_2 - H_2O solution was prepared by boiling a 3 M HNO_3 - I_2 solution and passing the vapors through CuO at 750°C prior to condensing the I_2 and water. Aliquots of this solution were then added to $\text{Hg}(\text{NO}_3)_2$ - HNO_3 solutions so that the resulting solution composition was 0.5 M $\text{Hg}(\text{NO}_3)_2$ --8 M HNO_3 -- 2.6×10^{-4} M I_2 ; these solutions were then sparged to determine the rate of iodine evolution. In one test series, the $\text{Hg}(\text{NO}_3)_2$ - HNO_3 solution used was prepared from ordinary distilled water. In the second series, an attempt was made to eliminate all organic impurities in the mercury solution by using water that had been passed through CuO at 750°C and condensed; also, after addition of the $\text{Hg}(\text{NO}_3)_2$ and HNO_3 to this water, the resulting solution was ozonized and then sparged briefly with air to eliminate the excess ozone.

Results of the tests are shown in Fig. 10-7. In the first test series with solution prepared with ordinary distilled water, the iodine liquid/gas distribution coefficient, D_G^L , was 1.45×10^7 when the 2-hr sparge test was started within a few minutes after mixing of the solutions. Aging the solution for 21 hr increased the D_G^L value (decreased iodine evolution) by a factor of about 2. With the "pure" solution, the amount of iodine volatilized was a factor of 1.6 to 2.5 lower than that from the "impure" solution at equivalent aging times. In both cases, iodine evolution appeared to reach a maximum a few hours after preparation of the solution.

A test was run in which an iodine reducing agent (0.02 M Na_2SO_3) was added to the "impure" mercury solution before addition of the I_2 - H_2O solution; sparging was started immediately after mixing of the solutions. The iodine in the traps was below the level of detection ($D_G^L > 10^8$). This is consistent with previous observations that formation of organic iodides is less likely to occur when the iodine is in its lowest valence state.

ORNL DWG 72-13887R1

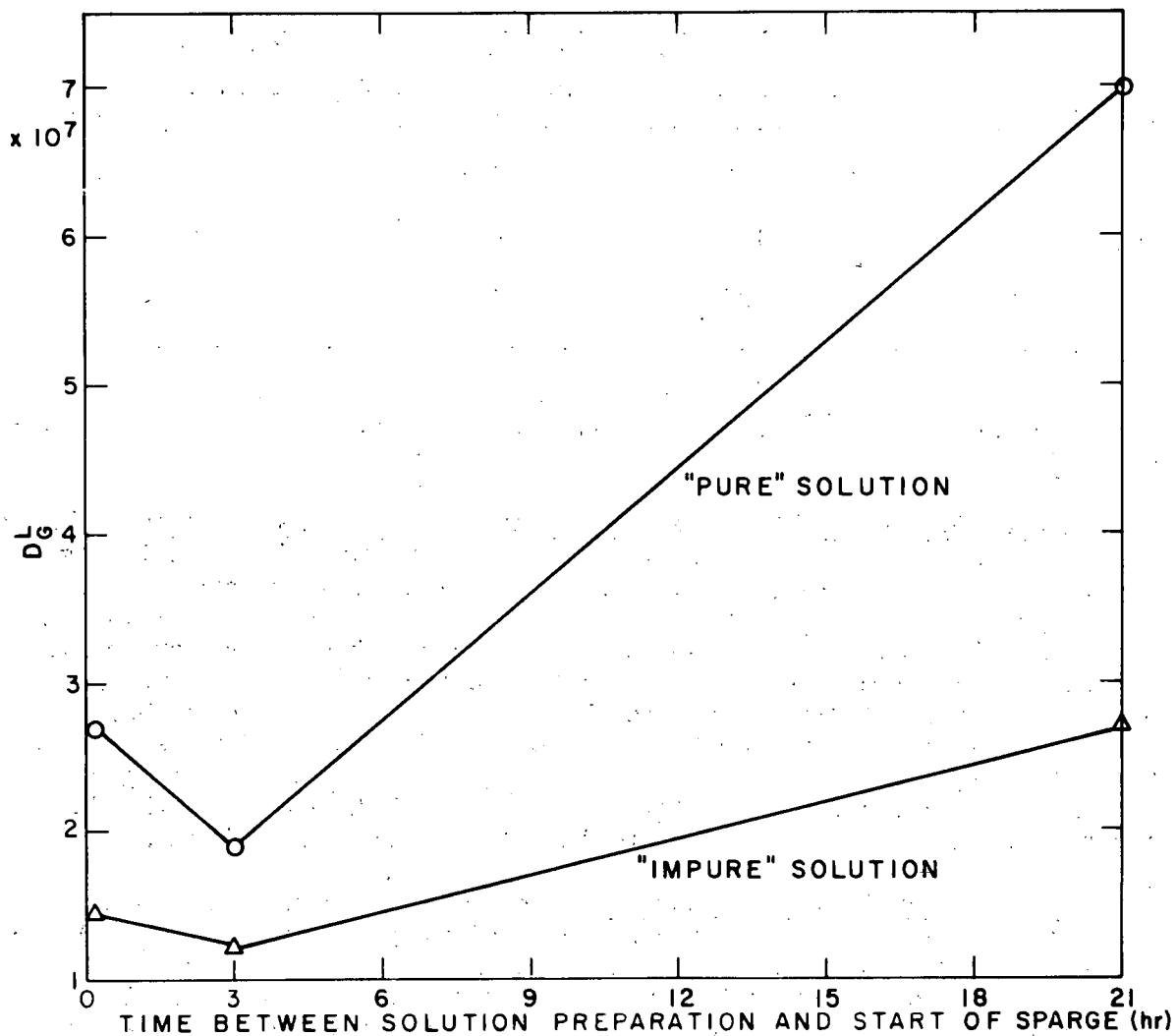


Fig. 10-7. Effect of Solution Purity and Aging Time on Evolution of Iodine from 0.5 M $\text{Hg}(\text{NO}_3)_2$ --8 M HNO_3 Solutions. Solution (50 ml) sparged 2 hr with 150 cc/min of air at $\sim 25^\circ\text{C}$.

Study of the effect of acid type on iodine evolution showed approximately equivalent results for nitrate and sulfate solutions; significantly less iodine was volatilized from acetate solutions. The amount of iodine volatilized from the nitrate and sulfate solutions decreased by a factor of about ten on aging of the solutions for 20 days:

System	$\frac{D^L}{G}$		
	Time Between Solution Preparation and Start of 2-hr Sparge		
	10 min	2 days	20 days
Nitrate	7.5×10^7	2.0×10^7	6.7×10^8
Sulfate	5.3×10^7	3.7×10^7	8.7×10^8
Acetate	1.1×10^8	1.4×10^8	--

In these tests the Hg^{2+} concentration was 0.2 M and the acid concentration was 4 N.

Methyl Iodide Scrubbing Runs in Simulated Bubble-Cap Columns. — Eight runs were made in two glass bubbler columns of the design shown in Fig. 10-8. Using 0.4 M $Hg(NO_3)_2$ -- 10 M HNO_3 in a 1-in.-diam column, the DF per stage was 2.5 at a gas flow of about 13 ft/min and 4.07 at a gas flow of 6.5 ft/min (Table 10-8). Appreciably higher efficiencies were obtained in the 1.6-in.-diam column at equivalent gas flow rates, undoubtedly because the gas was dispersed into the solution through smaller holes and at a greater solution depth. As shown in Fig. 10-9, the stage value of DF-1 (see equation 1, p. 31) was inversely proportional to the gas flow rate. Stage aqueous samples in these runs indicated that the decontamination performance was approximately the same in each stage.

Thermal Stability of Mercuric Iodate. — In the mercury scrubbing process flowsheet, the mercuric nitrate solution is circulated in closed cycle. Accumulated iodine is taken off from the system by heating a small fraction of the recycle stream to concentrate and precipitate the iodine as mercuric iodate. Conceivably, the iodine could be stored in this form; alternatively, it could be converted to sodium iodate by reaction with caustic, allowing complete recycle of the mercury. A mercuric iodate product was prepared from a volume of scrub solution. The precipitate was washed with water and air dried; analysis of the precipitate showed 36.7% Hg and 45.8% I, confirming that it was $Hg(IO_3)_2$. A thermal gravimetric analysis showed no decomposition of the sample until the temperature reached about 520°C, at which point, there was a rapid loss of weight.

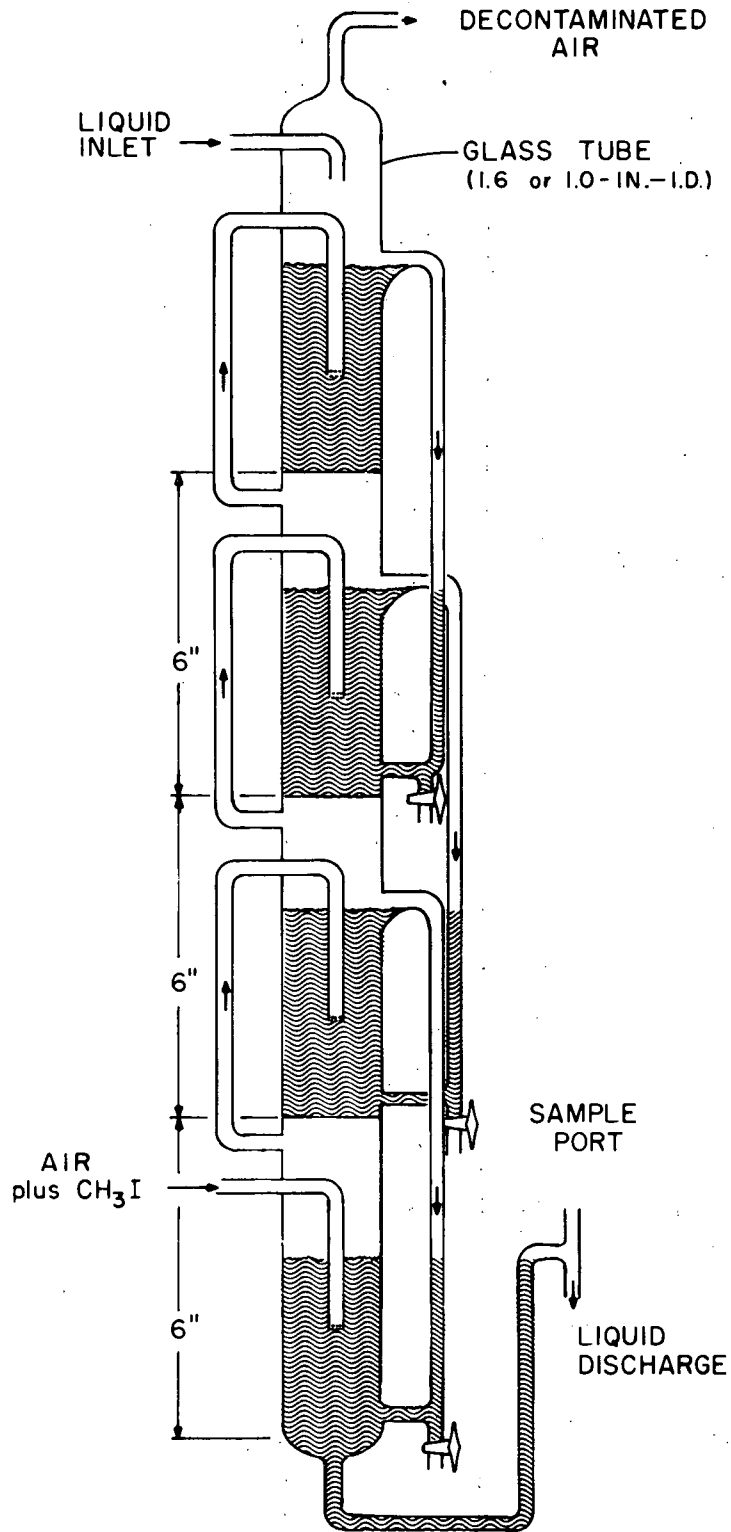


Fig. 10-8. Simulated Bubble-Cap Column Used in Scrubbing Methyl Iodide from Air with Mercury Solutions (additional details of design are given in footnotes of Table 10-8).

Table 10-8. Scrubbing of Methyl Iodide from Air in Simulated Bubble-Cap Columns with HNO_3 - $\text{Hg}(\text{NO}_3)_2$ Solutions at 25°C

Run	Solution		Column Diameter (in.)	No. of Stages	Gas Flow		DF	DF per Stage
	HNO_3 (M)	Hg^{2+} (M)			liter/min	ft/min		
1	10	0.4	1.0 ^a	3	2.05	13.3	15.5	2.5
2	10	0.4	1.0 ^a	3	1.94	12.6	21.3	2.77
3	10	0.4	1.0 ^a	3	1.0	6.5	67.5	4.07
4	10	0.4	1.6 ^b	4	3	7.6	1068	5.71
5	10	0.4	1.6 ^b	4	5	12.7	405	4.49
6	10	0.4	1.6 ^b	4	7	17.8	122	3.32
7	10	0.2	1.6 ^b	4	5	12.7	71.7	2.90
8	14	0.2	1.6 ^b	4	5	12.7	3.3×10^4	13.5

^aLiquid flow of 1 ml/min; solution depth was 2.5 in.; gas dispersed at ~1.5-in. depth through twelve 0.05-in.-diam holes; pressure drop across the three stages was ~3.5 in. of water at a gas flow rate of 2 liters/min and ~5.7 in. at 1 liter/min.

^bLiquid flow rate of 10 ml/min; solution depth was 4 in.; gas dispersed at ~2.5-in. depth through twenty-one 0.03-in.-diam holes.

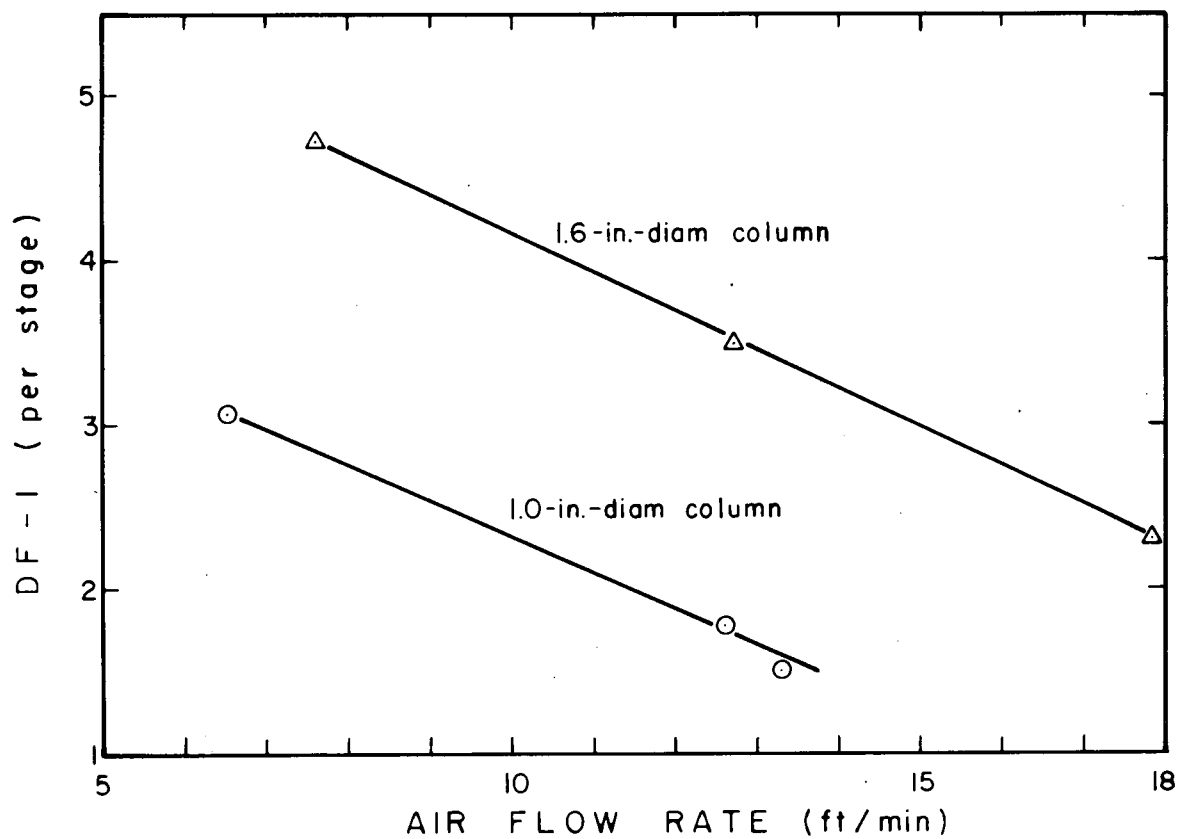


Fig. 10-9. Data for Bubble-Cap Column Runs on Scrubbing Methyl Iodide from Air with 0.4 M $\text{Hg}(\text{NO}_3)_2$ --10 M HNO_3 (gas dispersal method for each column is described in footnotes of Table 10-8).

References for Sect. 10

1. W. E. Unger et al., IMFBR Fuel Cycle Studies Progress Report for September, 1973, No. 43, Sect. 10.1, ORNL-TM-4016.
2. W. E. Unger et al., IMFBR Fuel Cycle Studies Progress Report for August 1973, No. 42, Sect. 10.1, ORNL-TM-3993.

11. ENGINEERING STUDIES (TASK 11)

(A. R. Irvine)

The purpose of this task is to examine the overall problem of LMFBR spent fuel recovery plant design and to relate the individual problems involved in fuel recovery to the overall problem and to the other individual problems. Individual problems to be evaluated range from special problems in safety and containment (which are peculiar to reprocessing of LMFBR spent fuel) to equipment design and operational procedures.

Integrated Engineering Facility Study (Task 11.3)

(E. L. Nicholson, S. D. Clinton, F. E. Harrington,
L. B. Shappert, J. B. Ruch, O. O. Yarbrow)

Work has continued on process definition, process criteria, and design selection of equipment related to the above subject. This is being accomplished by examining the various available options for each of the process steps for applicability to a production scale (5 T/D) facility. When the work is completed, it will be issued as a topical report. Drafts have been prepared of the sections dealing with fuel disintegration (shearing), voloxidation, and dissolution. We expect to include in the report recommendations pertaining to the work required for development of an applicable LMFBR fuel recovery plant.

3

•

•

•

•

•

•

•

INTERNAL DISTRIBUTION

- | | | | |
|-----|-------------------|--------|-----------------------------------|
| 1. | R. D. Ackley | 34. | A. H. Kibbey |
| 2. | R. E. Blanco | 35. | B. B. Klima |
| 3. | J. O. Blomeke | 36. | R. E. Leuze |
| 4. | W. D. Bond | 37. | B. Lieberman |
| 5. | R. E. Brooksbank | 38. | A. L. Lotts |
| 6. | K. B. Brown | 39. | R. S. Lowrie |
| 7. | F. R. Bruce | 40. | R. E. MacPherson, Jr. |
| 8. | W. D. Burch | 41. | W. T. McDuffee |
| 9. | G. I. Cathers | 42. | J. P. Nichols |
| 10. | S. D. Clinton | 43. | E. L. Nicholson |
| 11. | H. E. Cochran | 44. | J. R. Parrott |
| 12. | C. F. Coleman | 45. | A. M. Perry |
| 13. | L. T. Corbin | 46. | R. L. Philippone, RDT at ORNL |
| 14. | D. J. Crouse | 47. | R. H. Rainey |
| 15. | F. L. Culler, Jr. | 48. | A. D. Ryon |
| 16. | W. Davis, Jr. | 49. | L. B. Shappert |
| 17. | V. A. DeCarlo | 50. | J. W. Snider |
| 18. | D. E. Ferguson | 51. | M. J. Stephenson, ORGDP |
| 19. | L. M. Ferris | 52. | D. B. Trauger |
| 20. | C. L. Fitzgerald | 53-54. | W. E. Unger |
| 21. | J. D. Flynn | 55. | C. D. Watson |
| 22. | M. H. Fontana | 56. | A. M. Weinberg |
| 23. | H. W. Godbee | 57. | G. A. West |
| 24. | H. E. Goeller | 58. | M. E. Whatley |
| 25. | J. H. Goode | 59. | R. G. Wymer |
| 26. | A. T. Gresky | 60. | O. O. Yarbro |
| 27. | W. S. Groenier | 61. | H. C. Young |
| 28. | P. A. Haas | 62. | Laboratory Records, RC |
| 29. | W. O. Harms | 63-64. | Central Research Library |
| 30. | F. E. Harrington | 65. | Document Reference Section |
| 31. | D. E. Horner | 66-75. | Laboratory Records |
| 32. | A. R. Irvine | 76. | ORNL Patent Office |
| 33. | P. R. Kasten | 77. | Nuclear Safety Information Center |

EXTERNAL DISTRIBUTION

78. Research and Technical Support Division, AEC-ORO
79. RDT Senior Site Representative, D. F. Cope, ORNL
80-81. Director, Division of Reactor Development & Technology
U. S. Atomic Energy Commission
Washington, D. C. 20545
82-276. Given distribution as shown in TID-4500 under UC-79c -
Fuel Recycle Category.